Article

SOURCE
DATA

TRANSPARENT
PROCESS

THE
EMBO
JOURNAL

The tRNA pseudouridine synthase TruB1 regulates the maturation of let-7 miRNA

Ryota Kurimoto[1], Tomoki Chiba[1], Yoshiaki Ito[1,2], Takahide Matsushima[1], Yuki Yano[1], Kohei Miyata[3], Yuka Yashiro[4], Tsutomu Suzuki[5] (iD), Kozo Tomita[4] & Hiroshi Asahara[1,6,*] (iD)

Abstract

Let-7 is an evolutionary conserved microRNA that mediates post-transcriptional gene silencing to regulate a wide range of biological processes, including development, differentiation, and tumor suppression. Let-7 biogenesis is tightly regulated by several RNA-binding proteins, including Lin28A/B, which represses let-7 maturation. To identify new regulators of let-7, we devised a cell-based functional screen of RNA-binding proteins using a let-7 sensor luciferase reporter and identified the tRNA pseudouridine synthase, TruB1. TruB1 enhanced maturation specifically of let-7 family members. Rather than inducing pseudouridylation of the miRNAs, high-throughput sequencing crosslinking immunoprecipitation (HITS-CLIP) and biochemical analyses revealed direct binding between endogenous TruB1 and the stem-loop structure of pri-let-7, which also binds Lin28A/B. TruB1 selectively enhanced the interaction between pri-let-7 and the microprocessor DGCR8, which mediates miRNA maturation. Finally, TruB1 suppressed cell proliferation, which was mediated in part by let-7. Altogether, we reveal an unexpected function for TruB1 in promoting let-7 maturation.

Introduction

MicroRNAs (miRNA) are short non-coding RNAs of about 22 bases that regulate gene expression by inhibiting either the stability of target mRNAs or protein synthesis in association with Argonaute (AGO) family proteins (Lee *et al*, 1993; Wightman *et al*, 1993). Lin-4 and let-7 were the first reported miRNAs in *Caenorhabditis elegans* (Lee *et al*, 1993; Reinhart *et al*, 2000). Since then, more than 1,500 conserved miRNAs have been identified across many species including mammals (Ambros, 2004). The expression and maturation of miRNAs are tightly regulated by multi-step mechanisms involving protein-RNA associations with enzymatic activities and molecular shuttling, specifically: (i) Pol-II-mediated primary miRNA (pri-miRNA) transcription (Cai *et al*, 2004; Lee *et al*, 2004), (ii) Drosha/DiGeorge syndrome critical region 8 (DGCR8)-mediated processing producing a precursor-miRNA (pre-miRNA) in the nucleus (Lee *et al*, 2003; Denli *et al*, 2004; Gregory *et al*, 2004; Han *et al*, 2004; Landthaler *et al*, 2004; Zeng *et al*, 2005), (iii) nuclear export of pre-miRNA by exportin-5 (Yi *et al*, 2003; Bohnsack *et al*, 2004; Lund *et al*, 2004), (iv) additional cleavage by the RNase III enzyme Dicer in the cytoplasm (Grishok *et al*, 2001; Hutvágner *et al*, 2001; Ketting *et al*, 2001; Knight & Bass, 2001), and (v) incorporation into the RNA-induced silencing complex (RISC) with AGO family proteins to generate the final miRNA (Mourelatos *et al*, 2002). Although the first transcription step for pri-miRNA expression can be driven by transcription factors and RNA Pol-II as well as mRNA, the following maturation steps, (ii–v), are also critical and unique to miRNA biogenesis and dynamics (Krol *et al*, 2010; Ha & Kim, 2014; Bartel, 2018).

The comparison of gene expression in tumor tissues showed discrepancies in the levels of miRNAs and their pri-miRNAs (Thomson *et al*, 2006). In particular, mutually exclusive and reciprocal regulation between the let-7 miRNA and the RNA-binding protein (RBP) Lin-28 at these maturation process have been well demonstrated in ES cells, *C. elegans*, and cancer pathology (Heo *et al*, 2008; Newman *et al*, 2008; Piskounova *et al*, 2008; Viswanathan *et al*, 2008; Chang *et al*, 2009). Lin28A/B specifically binds to the preE loop sequence of pri-/pre-let-7 and suppresses the processing of let-7 by causing oligo-uridylation of the let-7 precursor through TUT4/7 activity (Heo *et al*, 2008; Piskounova *et al*, 2011). Based on these fundamental findings, the factors mediating let-7 multi-step regulation, which may be critical for various biological and pathological events, have been extensively explored by several approaches (Newman *et al*, 2008; Trabucchi *et al*, 2009; Treiber *et al*, 2017). Recently, it has been reported that METTL1 promotes processing of microRNA let-7 by m7G methylation (Pandolfini *et al*,

2019). However, to date, only a few factors have been shown to regulate let-7 family-specific maturation (Newman *et al*, 2008; Trabucchi *et al*, 2009; Michlewski & Caceres, 2010; Choudhury *et al*, 2014).

Taking advantage of the completion of genome-wide comprehensive full-length cDNA libraries (Chanda *et al*, 2003; Conkright *et al*, 2003; Iourgenko *et al*, 2003; Huang *et al*, 2004; Liu *et al*, 2005), we and others successfully developed cell-based screening systems to quantify miRNA targets and functions, including destabilization of target mRNA and suppression of protein synthesis (Wolter *et al*, 2014, 2015; Ito *et al*, 2017). Here we applied the above strategy and introduced a new cell-based screening to identify genes that regulate let-7 miRNA by using a luciferase reporter assay with a set of expression plasmid libraries mainly encoding proteins with RNA-binding properties. We identified a new regulatory mechanism: TruB1, an RNA-modifying enzyme, selectively regulates let-7 levels in an enzymatic activity-independent manner.

Results

Functional screening to detect RNA-binding proteins (RBPs) that promote let-7 expression

We developed a cell-based, functional screen using an expression plasmid library and a let-7 sensor reporter to identify proteins that regulate let-7 biogenesis. This type of screen enables the identification of proteins that regulate endogenous let-7 levels, as opposed to other aspects of let-7 biology, such as binding, which is assayed using affinity-based (pull-down) screens. The gain-of-function format also enables the identification of regulatory factors that may cause lethality under loss of function conditions, such as with Crispr-Cas9 or RNAi-KD screens. The let-7 sensor reporter was designed to monitor let-7 expression levels by inserting a let-7a target site into the luciferase 3′UTR region driven by the SV-40 promoter in pLuc2 plasmids (Fig 1A). Thus, luciferase activity is repressed in the presence of let7 miRNA (Fig EV1A). In this screen, we focused on identifying molecules directly regulating the miRNA maturation process; thus, we prepared a sib-selection library covering molecules annotated with RNA-binding protein (RBP) features from the Center for Cancer systems Biology (CCSB)-Broad Lentiviral overexpression library (Yang *et al*, 2011). As many zinc-finger-proteins have not been directly tested for their RNA or DNA binding preference, the genes with zinc-finger domains were also included in the sib-selection library. Ultimately, 1,469 genes were selected and prepared for the screening. This library was transfected into HEK293FT cells, along with the let-7 sensor reporter. If let-7 maturation is inhibited by coexpression of one of the cDNAs in the RBP library, expression of the luciferase reporter would be induced. As a positive control for the assay, we overexpressed Lin28A from the same backbone plasmid transfection along with the let-7 sensor reporter with or without overexpression of pri-let-7a in HEK293FT cells. This significantly promoted luciferase activity reflecting reduction of endogenous let-7 expression (Fig 1B). Next, we screened the 1,469 genes in our library utilizing the luciferase assay with the let-7 sensor reporter in HEK293FT cells seeded into 384-well plates (Fig 1C). pRL-SV40 Renilla luciferase activity was used as a transfection efficiency control. We only included genes that did not

change the luciferase activity of the let-7 sequence minus the reporter (0.5 <, > 2.0) (results are shown in Table EV1). Of these, we found that overexpression of 259 genes significantly reduced relative luciferase activity (< 0.50) compared with the GFP expression plasmid control (Fig 1D), indicating that they potentially promote let7 miRNA maturation. From the top five hits, we performed a larger scale (96-well plate) luciferase reporter assay for validation, whereby four of the top five genes reproducibly repressed the luciferase activity of the let-7 sensor (Fig 1E). To confirm the effect on endogenous let-7a expression, we examined the expression levels of a panel of ten miRNAs including let-7a by qPCR. Consistent with the screening results, overexpression of all of the top five candidate genes significantly promoted endogenous let-7a expression. Only TruB1 selectively induced let-7 expression but did not increase expression of the other miRNAs, whereas the other four hits, SF3A3, LARP7, GLTSCR2, and EF1E1, also increased the other miRNAs (Fig 1F). This suggests the specific promotion of let-7 biogenesis by TruB1. TruB1 is among the RNA-modifying enzymes that mediate pseudouridylation of tRNA. TruB1 has also recently been shown to regulate mRNA via pseudouridylation (Schwartz *et al*, 2014; Safra *et al*, 2017), but, to date, there has been no reported function of TruB1 in miRNA biogenesis.

TruB1 selectively promotes the expression of the let-7 family

Although a few proteins, such as Lin28A/B, KSRP, hnRNPA1, have been shown to be involved in the biogenesis of a specific set of miRNAs, most other miRNA regulators act without specificity, or their miRNA selectivity remains unclear. To test whether TruB1-dependent let-7 promotion is specific for the let-7 family, as our preliminary results suggested, we comprehensively analyzed the effect of TruB1 knockdown by siRNA on miRNA biogenesis in HEK293FT cells by TaqMan array. TruB1 knockdown downregulated the expression of four let-7 family members (let-7a, b, c and g) (Figs 2A and EV1B, Table EV2). These data were further confirmed by large scale TaqMan PCR for miRNA and Northern blotting (NB) in HeLa cells, revealing that almost all endogenous let-7 family genes were significantly downregulated upon TruB1 knockdown (Fig 2B–D). We confirmed these findings in A549 cells (Fig EV1C). Although there was some variation in the effects observed, the large scale qPCR experiments revealed a similar trend for each member of the let-7 family upon TruB1 knockdown in three cell types (HEK293FT cells, HeLa cells, and A549 cells). Even the members that did not show a statistically significant difference still showed a tendency to decline. TruB1 knockdown also decreased the level of pre-let-7a1 (Fig 2B). In contrast, TruB1 knockdown increased the levels of endogenous, immature, primary let-7 (Fig 2E). When we measured the processing rate, TruB1 knockdown significantly decreased the processing rate both of pri-to-pre and pre-to-mature processing. These results indicate that TruB1 promotes let-7 family miRNA biogenesis specifically at their maturation step, rather than at the transcriptional level.

TruB1 promotes miRNA processing independently of its enzymatic activity

We analyzed whether let-7 regulation by TruB1 is dependent on the pseudouridine enzyme activity of TruB1. Critical residues involved

A

Sensor (-) Luc2

Sensor (+) Luc2

let-7a antisense 5'…AACTATACAACCTACTACCTCA…

| | | | | | | | | | | | | | | | | | | | | | |

let-7a 3'…UUGAUAUGUUGGAUGAUGGAGU…

B

C

Gene expression library
1,469 genes
384 well plate x 7

48hr

← let-7 sensor

← HEK293FT cells

Luciferase reporter assay

D

Relative luciferase activity (/Ctrl)

E

Relative luciferase activity (/Ctrl)

F

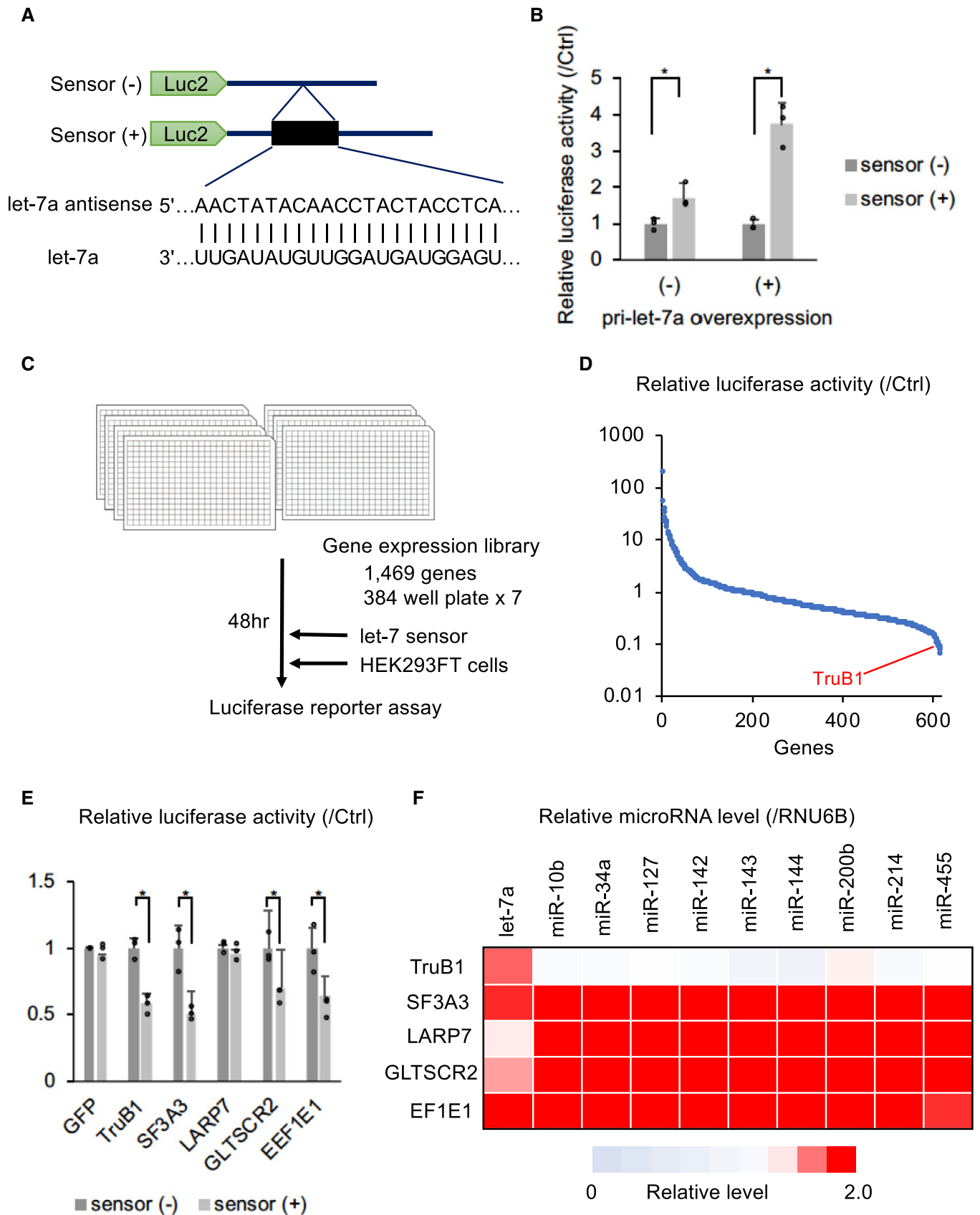Relative microRNA level (/RNU6B)

Figure 1.

Figure 1. Functional screen using a luciferase reporter assay to identify RBPs inducing let-7-expression.

A   Design of the let-7 sensor reporter and sequence of let-7a. Sensor (+) vector has the antisense sequence of let-7a inserted into the 3′UTR of the luciferase gene.
B   Relative luciferase activity of the let-7 sensor reporter (sensor (+)) or the negative control sensor (−) reporter contransfected with pLX-Lin28A in HEK293FT cells with or without pcDNA-pri-let-7a transfection. Error bars show SD; $n = 3$. Significance was assessed using 2-tailed Student's t-test, < 0.05*.
C   The screening model. A screening in 384-well plates with a library of 1,469 genes was performed.
D   Screening results: relative luciferase activity of each gene in the library. Only genes that did not affect the luciferase activity of the sensor (−) reporter (0.5 <, > 2.0) were analyzed. The full results of the screen are also in Table EV1.
E   Relative luciferase activity of the sensor (+) reporter or sensor (−) reporter induced by expression vectors of the top 5 genes identified in the screen or the GFP vector in HEK293-FT cells. Error bars show SD; $n = 3$. Significance was assessed using 2-tailed Student's t-test, 0.05*.
F   Heat map of relative miRNA expression of various miRNAs in HEK-293FT cells transfected with expression vectors of the top 5 genes from the screen, or the ctrl (GFP) vector. Red color represents suppressed expression compared with ctrl (GFP). $n = 3$.

Source data are available online for this figure.

in enzymatic activity (D48, D90) and RNA-binding ability (K64) have been identified in *Escherichia coli* TruB (Wright *et al*, 2011; Friedt *et al*, 2014; Keffer-Wilkes *et al*, 2016). Given the TruB amino acid sequences for these enzyme activity and RNA-binding ability are highly conserved (Zucchini *et al*, 2003), we were able to insert mutations to modify the function of TruB1 by amino acid substitution. We generated two TruB1 mutants: Mt1, with inactivated enzyme activity, and mt2, with suppressed RNA-binding ability (Fig 3A). An *in vitro* enzymatic activity assay with a tRNA^phe substrate using the wt, mt1, and mt2 recombinant proteins showed that the pseudouridylation enzyme activities of both mt1 and mt2 were completely attenuated (Fig 3B). An EMSA study using recombinant proteins revealed a physical interaction between tRNA^phe and wt TruB1 and mt1, but not with mt2 (Fig EV2A). Next, we tested the function of these mutants in cells. Western blotting (WB) revealed that all proteins were overexpressed largely to the same levels (Fig EV2B). Overexpression of Wt and mt1 TruB1 significantly increased let-7a maturation, whereas mt2 did not (qPCR, NB). Although no change in pre-let-7 was observed, the processing rate of pre-to-mature was elevated by overexpression of Wt and mt1 (Fig 3C–E). These results suggest that promotion of let-7 maturation by TruB1 is independent of its enzyme activity, but dependent on RNA binding.

Next, we performed an *in vitro* enzyme assay to verify that let-7 could not be pseudouridylated by recombinant TruB1. Pseudouridine of tRNA^phe was clearly increased in the assay, whereas no pseudouridylation of pri-let-7 and another primary miRNA was observed (Fig 3F). We also examined the presence of pseudouridine directly by treatment with CMC (N-cyclohexyl-N0-(2-morpholinoethyl)carbodiimide metho-p-toluenesulfonate) followed by a primer extension assay. We monitored the position of the UTP using ddATP during a primer extension assay. If a band is found in CMC-

treated RNA that does not match the height of this UTP, it can be determined to be non-specific binding. Furthermore, the bands observed in non-CMC-treated RNA cannot indicate the presence of pseudouridine. Based on these conditions, the multiple thin bands found around 35 nt of CMC-treated RNA in let-7 are likely to be non-specific bands. The bands at the height of the UTP were also only of the same intensity as the other non-specific bands in let-7. In contrast, in tRNAs, a dense band of CMC-treated RNA consistent with the height of UTP was observed, indicating the presence of pseudouridine. These results indicate that pseudouridine is not present in endogenous let-7 (Figs 3G and EV2C). We also synthesized RI-labeled pri-let-7a1 in which pseudouridine was randomly introduced using UTP: pseudouridine at a ratio of 1:1. An *in vitro* processing assay using this labeled pri-let-7a1 showed that the presence of pseudouridine in pri-let-7a1 did not affect its processing (Fig EV2D and E). These results indicate that the regulation of let-7 by TruB1 does not depend on its enzyme activity.

TruB1 binds directly to primary let-7

To determine how TruB1 regulates let-7 processing, we first tested whether TruB1 binds to pri-let-7. RNA immunoprecipitation (RIP) assays revealed that overexpression of wt and mt1 TruB1 immunoprecipitated pri-let-7a1, whereas mt2 did not (Fig 4A). An EMSA study using recombinant proteins revealed a physical interaction between pri-let7a1 and wt and mt1 TruB1, but not with mt2 (Fig 4B). Furthermore, EMSA was performed using mutant RNA in which the loop structure of pri-let-7a1 was modified (loop mt). As a result, no binding to TruB1 was observed in the loop mt (Figs 4B and EV3A). To comprehensively survey the RNA-protein binding property under physiological conditions, we performed high-throughput crosslinking immunoprecipitation (HITS-CLIP)

Figure 2. TruB1 selectively promotes the expression of let-7 family miRNAs.

A   Volcano plot of TaqMan array showing the mean average expression and P-value of miRNA expression profiles between TruB1 KD and ctrl (scramble). $N = 3$. Significance was assessed using 2-tailed Student's t-test. MiRNAs suppressed (Relative expression TruB1 KD/ctrl < 0.8 and P-value < 0.1) are enclosed by the red square.
B   Northern blotting for let-7a, miR-34a, and RNU6B in HeLa cells with TruB1 KD or ctrl (siRNA).
C   Processing rates were quantified and normalized to ctrl based on hybridization intensities of (B). Significance was assessed using 2-tailed Student's t-test, < 0.05*.
D   Relative expression of let-7 family miRNAs and other miRNAs in HEK293FT cells with TruB1 KD or ctrl (siRNA) determined by qRT–PCR. Significance was assessed using 2-tailed Student's t-test, < 0.05*.
E   Relative expression of primary let-7 family miRNAs as in (D) determined by qRT–PCR. Significance was assessed using 2-tailed Student's t-test, < 0.05*.

Data information: All experiments were performed in triplicate. Error bars show SD.
Source data are available online for this figure.

A

TaqMan array (n=3)

let-7a
let-7c
let-7g
let-7b

p-value

Relative expression TruB1 KD / ctrl

B

Size marker / ctrl / TruB1 KD

200nt
100nt
80nt
50nt
20nt

pri-let-7a
pre-let-7a

Long expose

80nt
70nt
30nt
20nt

pre-let-7a
let-7a
RNU6B

Size marker / ctrl / TruB1 KD

pri-miR-34a
pre-miR-34a

miR-34a

C

Processing rate

*   *

pre/pri+pre   mat/pre+mat

■ Ctrl ■ TruB1 KD

D

■ Ctrl ■ TruB1 KD

mature-miR /RNU6B

* * * * * * *   *

a b c d e f g i miR-98

Number of let-7 families

mature-miR /RNU6B

10b 15a 34a 200c

Number of other microRNAs

E

■ Ctrl ■ TruB1 KD

pri-miR /GAPDH

* * * * * *   *   *   *

a1 a2 a3 b c d e f1 f2 g i miR-98
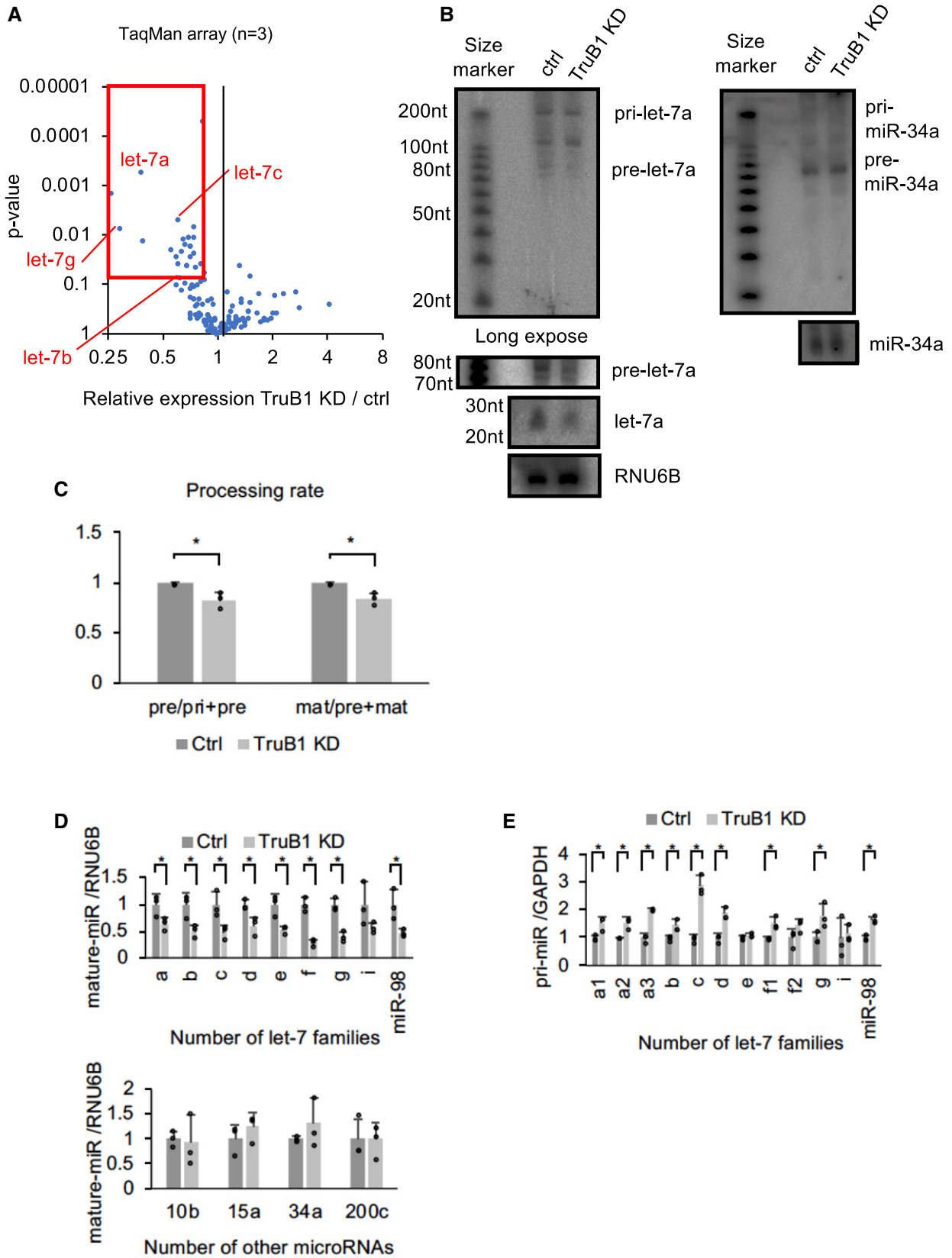
Number of let-7 families
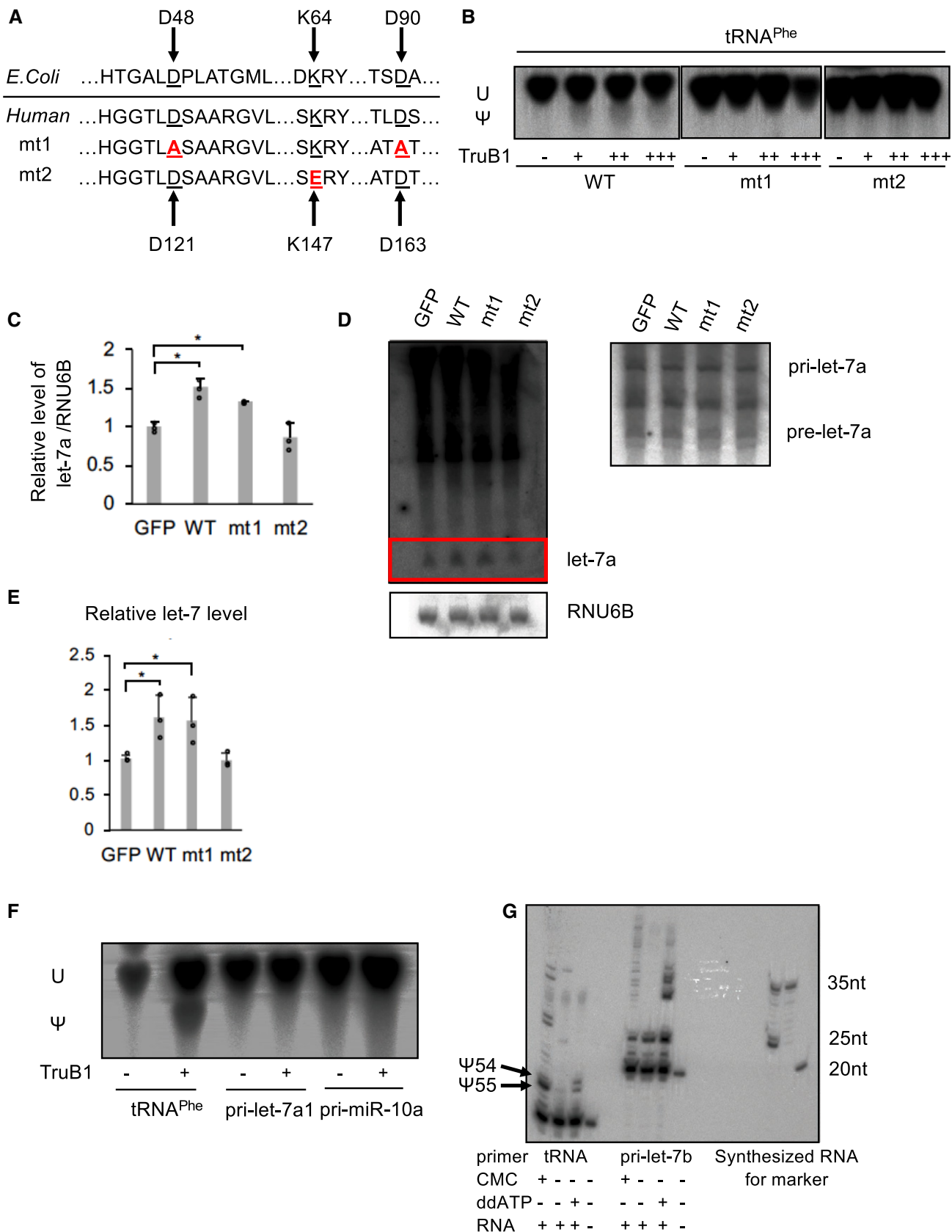
Figure 2.

Figure 3.

Figure 3. TruB1 promotes let-7 processing independently of its enzymatic activity.

A Amino acid sequences encoding for the enzyme activity and RNA-binding ability in *Escherichia coli* TruB and human TruB1 (Top). Design of mutant 1 (mt1) and mutant 2 (mt2) (bottom).

B *In vitro* enzyme activity assay. ^{32}p-UTP-labeled tRNA^{phe} were treated with recombinant TruB1, mt1, or mt2. The strong upper bands represent uridine (U), and the lower weaker bands represent pseudouridine (Ψ) on autoradiographs of the TLC plate.

C Relative miRNA expression of let-7a in HEK-293 cells infected with tetracycline-inducible expressing lentiviruses for TruB1, mt1, mt2, or GFP 5 days after doxycycline treatment, as determined by qRT–PCR. Significance was assessed using 2-tailed Student's *t*-test, < 0.05*.

D Northern blotting for let-7a and RNU6B in HeLa cells infected with lentiviruses encoding tetracycline-inducible expression of TruB1, mt1, mt2, or GFP, 5 days after doxycycline treatment.

E Hybridization intensities of (D) were quantified and normalized to ctrl (GFP). Significance was assessed using 2-tailed Student's *t*-test, < 0.05*.

F Pseudouridylation activity of TruB1 for tRNA and pri-miRNAs. ^{32}p-UTP-labeled tRNA^{phe}, pri-let-7a1, or pri-miR-10a were treated with recombinant TruB1. Upper bands represent uridine (U), lower bands represent pseudouridine (Ψ) in autoradiographs of the TLC plate.

G Location of pseudouridine sites detected by the CMC primer extension method. Total RNA purified from HEK-293FT cells were treated with CMC. CMC-treated RNA were reverse-transcribed with RI-labeled specific primers for tRNA^{phe} or pri-let-7b. ddATP was used for sequence control. Pseudouridines are indicated by black arrows.

Data information: All experiments were performed in triplicate. Error bars show SD.
Source data are available online for this figure.

using a cell line in which the 3xFLAG tag was knocked into the TruB1 N-terminal end by using the CRISPR/Cas9 system (Figs 4C and EV3B–F). This revealed the expected, but not previously shown, direct interaction between TruB1 and its known substrate tRNA (positive control). We also observed a physical interaction between TruB1 and pri-let-7a1 (Fig 4D, Table EV3). Direct binding sites were also found in other miRNA sequences, including miR-29b, miR-139, and miR-107 whose expression levels of their mature forms were also specifically decreased upon TruB1 KD in the TaqMan array (Fig 4E, Table EV3). Looking at the entire mapped reads, mRNA, lncRNA, and miRNA were detected in addition to tRNA (Fig 4F). It has been reported that mRNA is modified by TruB1, which is consistent with this result (Schwartz *et al*, 2014; Safra *et al*, 2017). When a read mapped to tRNA was extracted and motif analysis was performed, the sequence was similar to the pseudouridylation site reported for *Saccharomyces cerevisiae* PUS4 (Fig 4G), which is homologous with TruB1 (Fig 4H; Becker *et al*, 1997). Although reads mapped to let-7a1 bound mainly near the terminal loop, no sequence similar to the tRNA motif was found in the let7 loop sequence. tRNA and let-7 are similar in that they form a loop structure (Fig 4I). Thus, we considered that TruB1 binds to let-7 in a structure-dependent manner. Interestingly, the TruB1 binding site on pri-let-7a1 also contained the sequence (GGAG), which is a binding motif of the CCHC-zinc domain of Lin28A/B. This suggests that TruB1 and Lin28 both bind to the same stem-loop structure on *let-7* and may compete for binding.

TruB1 enhances the interaction between the microprocessor and primary let-7 and promotes microprocessing

The above results indicated that TruB1 directly binds to pri-let-7a1 under physiological conditions. To elucidate the function of this molecular interaction, we analyzed whether TruB1 was involved in the microprocessing step of miRNA biogenesis using an *in vitro* processing assay. RI-labeled pri-let-7a1 was incubated with a cell extract obtained from HEK293FT cells overexpressing different forms of TruB1. We used Dicer KD to clarify the band of pre-let-7. We found that the extract from cells overexpressing TruB1 promoted maturation of pri-let-7a1 into pre-/mature type of let-7a, whereas the extract from cells overexpressing mutant TruB1(mt2) did not. We also found that knockdown of endogenous TruB1 by siRNA inhibited maturation of pri-let-7a (Fig 5A and B). These results suggest that let-7a biogenesis is promoted at the level of conversion from the pri-miRNA to the pre-miRNA and from the pre-miRNA to the miRNA. DGCR8 is the microprocessor involved in the cleavage of pri-miRNA in the nucleus to form pre-miRNA. Thus, we tested the effect of TruB1 on the interaction between pri-let-7 and DGCR8 by RIP affinity assay using an antibody to endogenous DGCR8. Pri-let-7a1 was efficiently precipitated with DGCR8, as expected. However, TruB1 KD by siRNA treatment reduced this interaction between only pri-let-7a1 and DGCR8 (Figs 5C and EV4A), without affecting the expression level of DGCR8. Next, we performed immunoprecipitation in TruB1-Flag cells. When immunoprecipitated with an anti-Flag antibody, a slight DGCR8 band was

Figure 4. TruB1 binds to tRNA and primary let-7.

A RIP analysis of pri-let-7a1 and Flag-TruB1 from HEK-293FT cells. RNA was extracted from IP material and analyzed by qRT–PCR. HEK-293FT cells were infected with lentiviruses encoding tetracycline-inducible expression of TruB1, mt1, mt2, or GFP and treated with doxycycline. Error bars show SD; *n* = 3. Significance was assessed using 2-tailed Student's *t*-test, < 0.05*.

B EMSA of ^{32}p-ATP-labeled pri-let-7a1 or pri-let-7a1 loop mt mixed with recombinant TruB1, mt1, or mt2 at several doses. RNP: Ribonucleoprotein complexes.

C Design of Flag-labeled TruB1 knocked-in (KI) cells. HiBIT and 3 x Flag sequences were inserted into the N-terminus of the TruB1 gene in HEK-293FT cells.

D Sequencing clusters obtained from HITS-CLIP experiment. Left are for let-7 and right for tRNAs.

E Tag densities represented as dots. Density of miRNA clusters in HITS-CLIP were normalized by miRNA expression as determined by TaqMan array.

F The proportions of different types of mapped transcripts from the HITS-CLIP experiment.

G Sequence motifs from reads mapped to tRNAs from the HITS-CLIP experiment.

H TruB-modified site in tRNAs. Location of pseudouridine is colored in red.

I Sequence of the terminal loop in pri-let-7a1. Lin28B binding site is colored in red.
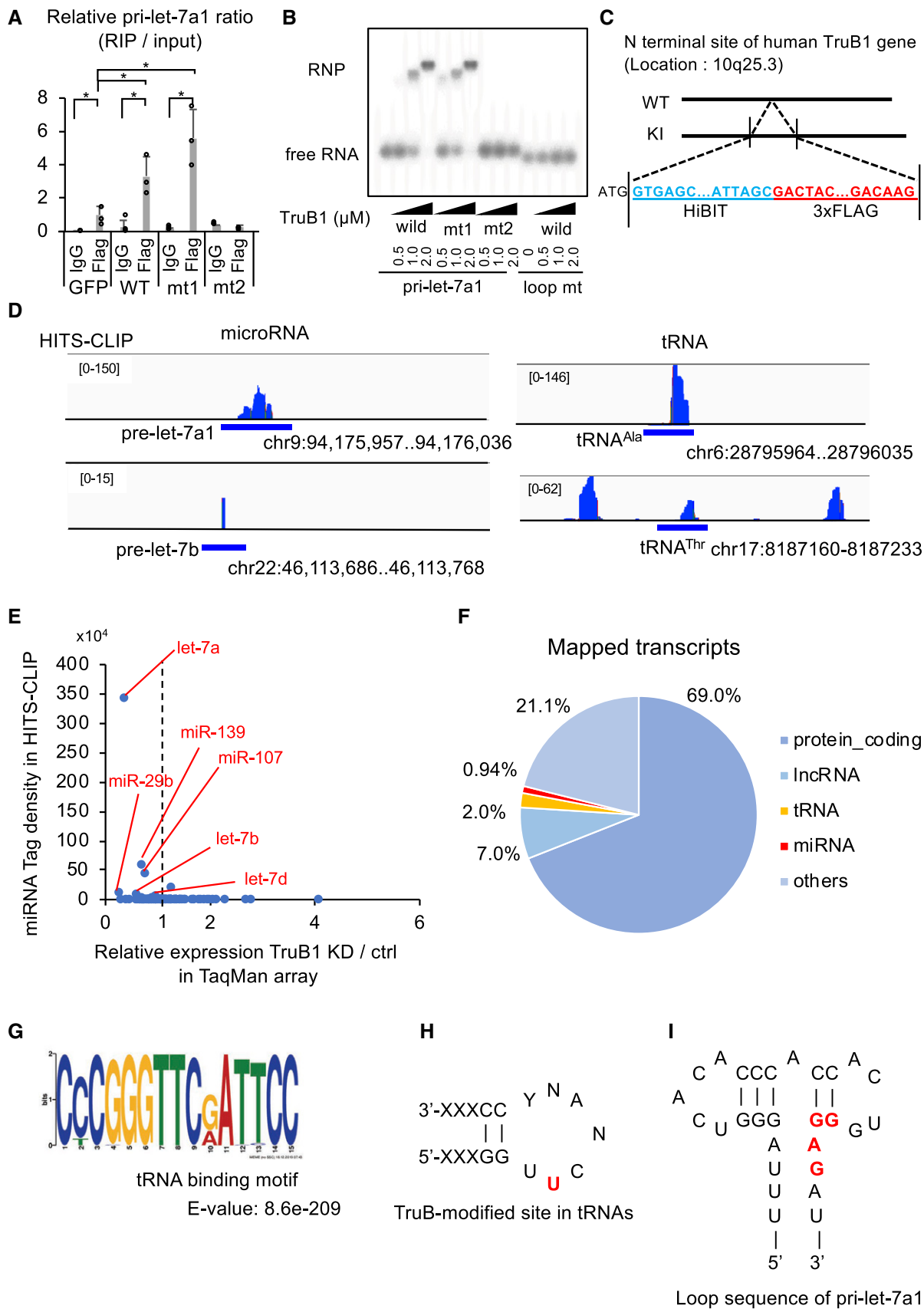
Source data are available online for this figure.

A Relative pri-let-7a1 ratio
(RIP / input)

B

RNP

free RNA

TruB1 (μM)

wild   mt1   mt2   wild

0.5 1.0 2.0 | 0.5 1.0 2.0 | 0.5 1.0 2.0 | 0.5 1.0 2.0

pri-let-7a1   loop mt

C N terminal site of human TruB1 gene
(Location : 10q25.3)

WT

KI

ATG GTGAGC...ATTAGC GACTAC...GACAAG
        HiBIT   3xFLAG

D

HITS-CLIP   microRNA

[0-150]

pre-let-7a1
chr9:94,175,957..94,176,036

[0-15]

pre-let-7b
chr22:46,113,686..46,113,768

tRNA

[0-146]

tRNA^Ala
chr6:28795964..28796035

[0-62]

tRNA^Thr chr17:8187160-8187233

E

x10^4

miRNA Tag density in HITS-CLIP

let-7a
miR-139
miR-107
miR-29b
let-7b
let-7d

Relative expression TruB1 KD / ctrl
in TaqMan array

F Mapped transcripts

21.1%   69.0%
0.94%
2.0%
7.0%

- protein_coding
- lncRNA
- tRNA
- miRNA
- others

G

tRNA binding motif
E-value: 8.6e-209

H

3'-XXXCC   Y N   A
        | | N
5'-XXXGG   U U C

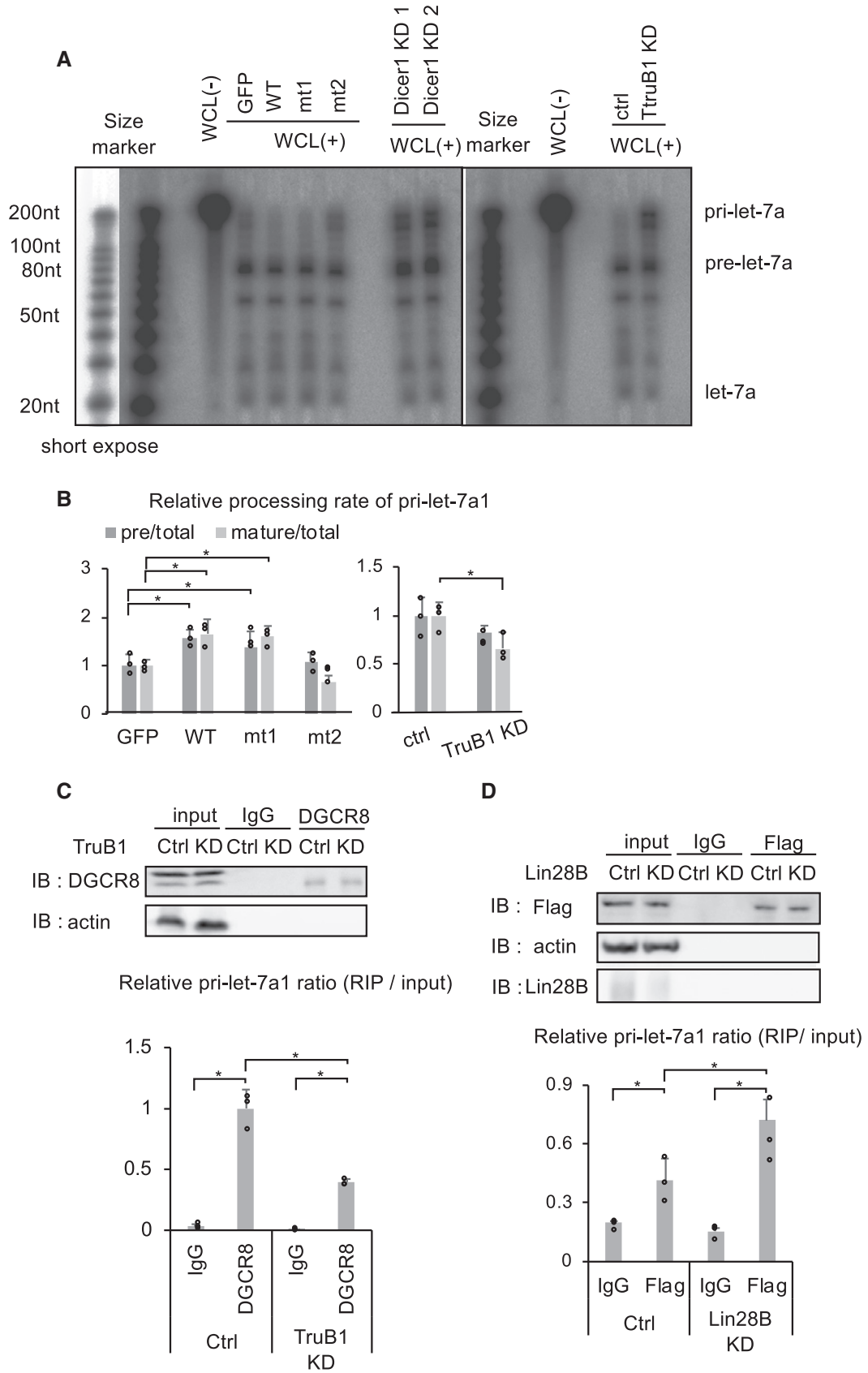TruB-modified site in tRNAs

I

Loop sequence of pri-let-7a1

Figure 5.

Figure 5. TruB1 promotes the microprocessing of primary let-7 and enhances binding of the microprocessor to primary let-7.

A   *In vitro* processing assay for RI-labeled pri-let-7a1. Autoradiographs of gels showing pri-let-7a1 treated with whole cell lysate (WCL) from HEK-293FT cells transfected with GFP, TruB1, mt1, or mt2 (overexpression, left), and TruB1 KD or ctrl (siRNA, right). Dicer KD was used to show the height of pre-let-7a1.

B   RI intensities of (A) were quantified and normalized to ctrl. Relative processing rate of pri-let-7a1 into pre-let-7a1 and mature-let-7a1 are shown. Significance was assessed using 2-tailed Student's *t*-test, < 0.05*.

C   RIP assay of pri-let-7a1 and DGCR8 from HEK-293FT cells. Western blotting for input or immunoprecipitate (IP) using anti-DGCR8 antibody and anti-actin antibody are shown on top. RNA was extracted from IP material and analyzed by qRT−PCR (bottom). Significance was assessed using 2-tailed Student's *t*-test, < 0.05*.

D   RIP assay of pri-let-7a1 and Flag-tagged TruB1 from HEK-293FT cells with Lin28B KD or ctrl (siRNA). Western blotting for input or IP material using anti-Flag antibody, anti-Lin28B antibody, and anti-actin antibody are shown on top. RNA was extracted from IP material and analyzed by qRT−PCR (bottom). Significance was assessed using 2-tailed Student's *t*-test, < 0.05*.

Data information: All experiments were performed in triplicate. Error bars show SD.
Source data are available online for this figure.

detectable by immunoblot with anti-DGCR8. Moreover, when immunoprecipitated with an anti-DGCR8 antibody, immunoblotting with an anti-Flag antibody detected TruB1 (Fig EV4B). Thus, TruB1 and DGCR8 were bound to each other. These data suggest that TruB1 is involved in enhancing complex formation between DGCR8 and pri-let-7a1. Next, we tested the potential interaction between TruB1/let-7 and Lin28B, which also binds to the pri-let-7a1 stem-loop region recognized by TruB1. In Lin28B knockdown cells, the ratio of TruB1-bound pri-let-7a1 over total pri-let-7a1 was increased, without altering TruB1 protein levels, as assessed by RIP (Figs 5D and EV4C). Thus, Lin28B inhibits the binding between TruB1 and pri-let-7a1.

TruB1 suppresses cell proliferation by promoting let-7 maturation

Finally, we examined the cellular function of this new TruB1/let-7 axis by analyzing cell growth. Let-7 coordinates cell proliferation by targeting a set of genes, including KRAS, which is a proto-oncogene (Johnson *et al*, 2005; Wang *et al*, 2013). To test whether TruB1 can affect KRAS expression via let-7 regulation, we generated a Luc-reporter plasmid comprising the let-7 target region of KRAS in its 3′UTR, and performed a luciferase reporter assay (Fig 6A). As a result, overexpression of wt TruB1 suppressed the luciferase activity of the KRAS reporter, whereas mt2 did not (Fig 6B). We also analyzed endogenous expression of KRAS by Western blotting and found that overexpression of TruB1 wt and mt1 decreased the expression of KRAS protein. In contrast, TruB1 KD increased the expression of KRAS (Fig 6C). Next, the effect of TruB1 overexpression on HEK-293FT cell growth was evaluated by real-time glo assay. Cell proliferation was significantly suppressed by TruB1 overexpression. To test whether this was mediated by let-7, we introduced RNAi to target the common seed sequence in the let-7 family. KD of the let-7 family partially rescued the suppressive effect of TruB1 overexpression on cell proliferation (Figs 6D and E, and EV5A). Taken together, these results indicate that cell proliferation can be regulated by the TruB1 and let-7 molecular cascade.

Discussion

In this study, we performed a systematic cell-based gain-of-function screen by combining an arrayed overexpression plasmid library and reporter system detecting let-7 expression and discovered a new

function for TruB1, which is a pseudouridine RNA-modifying enzyme (Fig 6F).

To date, various genes regulating miRNA maturation have been identified as co-immunoprecipitated factors from biotin-labeled miRNA hairpin, pri-miRNAs, or microprocessors (Chendrimada *et al*, 2005; Lee *et al*, 2006; Auyeung *et al*, 2013; Treiber *et al*, 2017); however, only a few of them have shown selectivity for miRNA biogenesis. In this study, we identified a set of molecules regulating let-7 biogenesis. Our strategy to use a cell-based and functional assay with an arrayed plasmid library has the following advantages: (i) The identified candidates are screened by their ability to regulate endogenous let-7 expression. Thus, the molecular function of the candidate proteins identified is already ensured, compared to a molecular affinity-based screening strategy, which only identifies binding. (ii) The use of a prepared set of genes from the library enables us to perform a quantitative and more efficient screen. All the raw data obtained in this approach are informative. (iii) The gain-of-function approach can identify factors that are necessary for cell survival, whereas loss of function screens, such as those using shRNA or CRISPR/Cas9, may be unable to detect them. This is particularly relevant when performing screens with molecules performing fundamental functions, such as let-7.

In our approach, we identified a set of proteins that significantly enhance endogenous let-7 expression. Among them, TruB1 is shown to play a critical role in let-7 specific miRNA maturation, whereas the other candidates did not show such selectivity. Among the other candidate genes, SF3A3 (Splicing Factor 3a Subunit 3) has been identified as one of the genes binding to the miRNA hairpin of let-7 (Treiber *et al*, 2017). However, the detailed mechanism of microRNA regulation by SF3A3 is unknown. There are no reports suggesting the direct involvement with microRNAs of the three other candidate genes.

TruB1 is a pseudouridine synthase (Zucchini *et al*, 2003), which is responsible for pseudouridylation, the first RNA modification found in tRNA and ribosomes (Cohn & Volkin, 1951; Charette & Gray, 2000). Pseudouridylation is thought to be required for modifying RNA structure by enhancing base-to-base stacking (Charette & Gray, 2000). TruB1 introduces pseudouridine at position 55 of tRNAs during the early stage of tRNA maturation (Becker *et al*, 1997; Zucchini *et al*, 2003). TruB1-mediated pseudouridine is also found in mRNA (Carlile *et al*, 2014; Schwartz *et al*, 2014; Li *et al*, 2015; Safra *et al*, 2017). Notably, our CLIP analysis for endogenous TruB1 revealed a physical association of TruB1 with a series of mRNAs, although the functional significance of these interactions and the potential pseudouridylation were not determined.
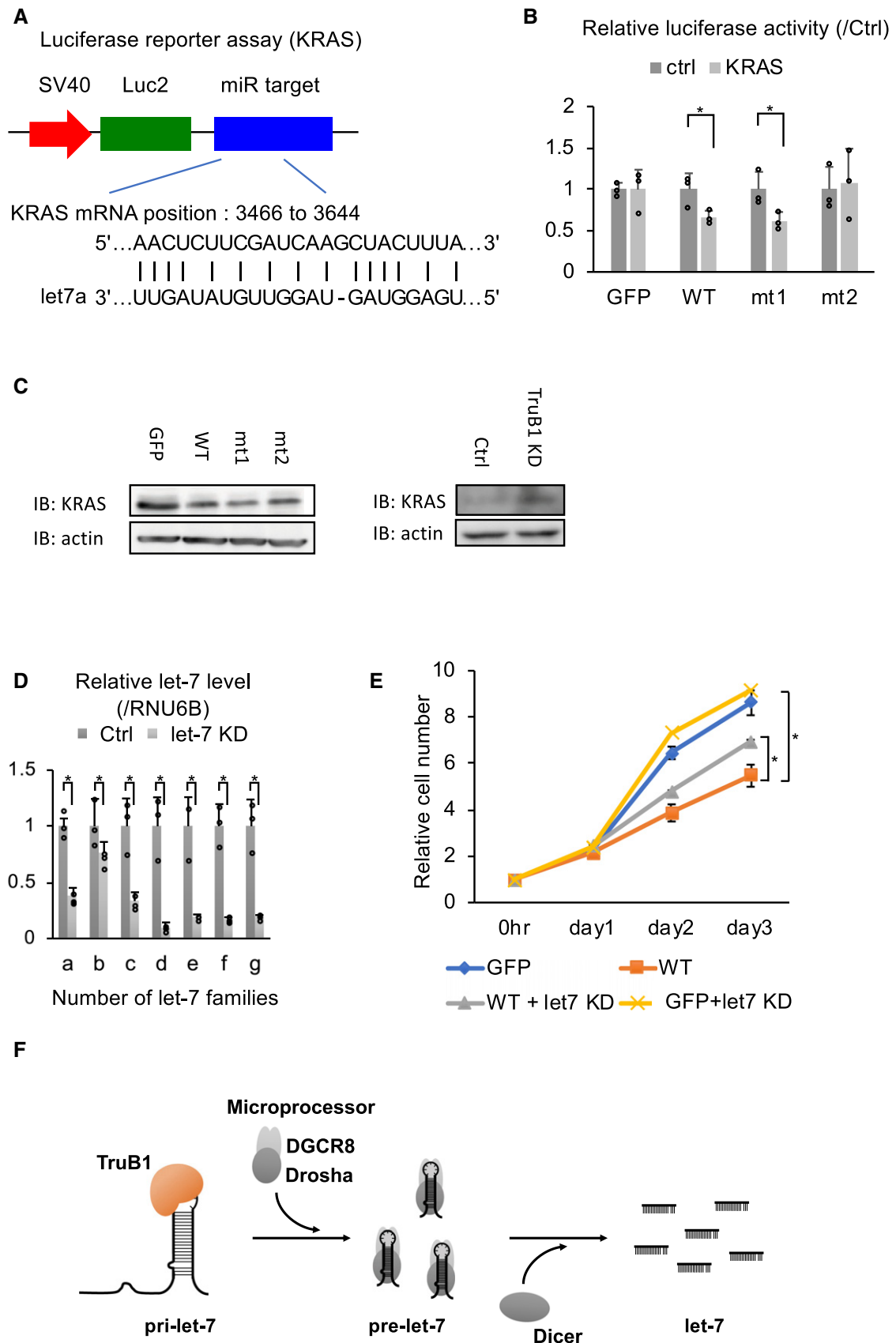
A

Luciferase reporter assay (KRAS)

SV40   Luc2   miR target

KRAS mRNA position : 3466 to 3644

5'…AACUCUUCGAUCAAGCUACUUUA…3'
     | | | | | | | | | | | | | | | | | | |
let7a 3'…UUGAUAUGUUGGAU - GAUGGAGU…5'

B

Relative luciferase activity (/Ctrl)

■ ctrl ■ KRAS

C

IB: KRAS

IB: actin

IB: KRAS

IB: actin

D

Relative let-7 level
(/RNU6B)

■ Ctrl ■ let-7 KD

Number of let-7 families

E

Relative cell number

◆ GFP   ■ WT
▲ WT + let7 KD   ✕ GFP+let7 KD

F

Microprocessor

TruB1   DGCR8
         Drosha

pri-let-7   pre-let-7   Dicer   let-7

Figure 6.

Figure 6. TruB1 suppresses cell growth by regulating let-7.

A   Design of luciferase reporter vector comprising the let-7 target region of KRAS mRNA (KRAS reporter).
B   Relative luciferase activity of KRAS reporter or Ctrl (empty) reporter in HEK293FT cells infected with lentiviruses expressing tetracycline-inducible TruB1, mt1, mt2, or GFP 5 days after doxycycline treatment. Significance was assessed using 2-tailed Student's t-test, < 0.05*.
C   Protein expression of KRAS. Protein expression was evaluated by Western blotting. Protein was isolated from HEK-293FT cells transfected with GFP, TruB1, mt1, or mt2 (overexpression, left), and TruB1 KD or ctrl (siRNA, right).
D   Relative expression of let-7 families determined by qRT–PCR in HEK-293FT cells with KD of let-7 family members or ctrl (using 2′-O-methylated antisense inhibitor). Significance was assessed using 2-tailed Student's t-test, < 0.05*.
E   Real-time glo assay for HEK293FT cells infected with lentiviruses expressing tetracycline-inducible TruB1 or GFP, 5 days after doxycycline treatment, with or without KD of let-7 family members. GFP: GFP without let-7 KD. WT: overexpression of wild-type TruB1 without let-7 KD. WT + let7 KD: WT: overexpression of wild-type TruB1 with let-7 KD. GFP + let-7KD: GFP with let-7 KD. Significance was assessed using 2-tailed Student's t-test, < 0.05*.
F   Schematic model for TruB1-dependent induction of let-7.

Data information: All experiments were performed in triplicate. Error bars show SD.
Source data are available online for this figure.

Escherichia coli TruB has been reported to function as a chaperone for tRNA that is not mediated by its enzymatic activity (Keffer-Wilkes *et al*, 2016). This reflects our finding that let-7 maturation promoted by TruB1 is also independent of its intrinsic pseudouridylation enzyme activity. It would thus be interesting to test whether the interactions we observed between TruB1 and mRNA are also independent of its pseudouridylation enzyme activity.

Examination of the crystal structures of bacterial TruB and tRNA reveals that the base of U55 in the TUC stem-loop structure near position 55 of the tRNA is flipped to bind to the catalytic site of TruB (Hoang & Ferre-D'Amare, 2001). In our HITS-CLIP, TruB1 was also bound to the stem-loop structure of let-7. Although the stem loop also exists in other miRNAs, only the let-7 stem loop is selectively regulated by binding of regulatory factors such as Lin28 and KSRP (Newman *et al*, 2008; Trabucchi *et al*, 2009). Consistent with this unique property of the let-7 stem loop, TruB1 also recognizes this region, which may cause physical competition among these specific regulators. It has been reported that the structure of RNA affects microprocessing with accessory proteins. For example, hnRNPA1 binds to the loop of pri-miR-18a and induces a relaxation at the stem. This relaxation at the stem facilitates Drosha-mediated processing of the specific microRNA clusters (Michlewski *et al*, 2008). The Dicer-TRBP complex has been reported to stabilize the stem structure of pre-let-7 before its cleavage reaction (Liu *et al*, 2018). These accessory proteins contribute to the structural changes in RNA and affect its processing. Like these accessory proteins, TruB1 also stabilizes the stem structure of tRNA and affects the enzymatic activity (Hoang & Ferre-D'Amare, 2001; Keffer-Wilkes *et al*, 2016). Thus, stabilization of RNA by accessory proteins may assist processors such as DGCR8. More detailed analyses are needed to determine the structural effects of TruB1 binding to let-7 and how it affects the microprocessing step of let-7 maturation.

TruB1 also bound to other miRNAs (miR-29b, miR-107, and miR-139), which are also downregulated upon TruB1 knockdown in our HITS-CLIP, suggesting a common regulatory mechanism. However, no common sequences matching in the loop structures of these three miRNAs were found. The binding consensus sequence of Lin28A/B, GGAG, was found in a stem-loop of miR-107 and miR-139 but not in miR-29b. However, the regulation of these miRNAs by LIN28A/B was not reported. The size of the loops was uniform, 11–14 nt. Moreover, it has been reported that KSRPs, which bind to the same stem-loop structure of let-7 as TruB1, promotes not only let-7 maturation but also several other microRNAs, including miR-

20a and miR-21 (Trabucchi *et al*, 2009). However, none of the three miRNAs were altered in KSRP (Trabucchi *et al*, 2009). Each of these three microRNAs has been reported to suppress tumor proliferation (Song *et al*, 2015; Sun *et al*, 2015; Sur *et al*, 2019). Further studies are needed in order to identify the common regulatory mechanism.

As a cell biological function of the TruB1 and let-7 interaction, we found that TruB1 controlled cell proliferation by promoting let-7 maturation. The expression level of TruB1 correlates with cancer progression and/or oncogenesis in prostate cancer and pancreatic cancer, suggesting that TruB1 could be involved in the pathogenesis of cancer (Fig EV5B–D; Edgar *et al*, 2002; Varambally *et al*, 2005a; Data ref: Varambally *et al*, 2005b; Pei *et al*, 2009a; Data ref: Pei *et al*, 2009b; Wang *et al*, 2015a; Data ref: Wang *et al*, 2015b). On the other hand, TruB2, which has the same enzyme activity site at TruB1, preferentially mediates pseudouridinylation of mitochondrial RNA and is essential for cell survival by controlling glycolysis (Arroyo *et al*, 2016; Antonicka *et al*, 2017). TruB KO *E. coli* were weaker than wild-type cells when they were co-cultured; however, this was not caused by decreased survival (Gutgsell *et al*, 2000). In this way, despite having highly conserved enzyme activity sites between species and homologs, their functions appear to be quite diverse.

PUS7, PUS10, DKC1, TruB1, TruB2, among others, are also pseudouridine synthases, and among them, PUS10 was recently reported to promote miRNA maturation also independently of its enzyme activity (Song *et al*, 2019). PUS10 introduces pseudouridine at position 55 of tRNA (Roovers *et al*, 2006), similar to TruB1, and position 54 of tRNA in archaea (Deogharia *et al*, 2019). PUS10 increases the affinity of microprocessors for various miRNAs and promotes their maturation (Song *et al*, 2019). However, these two pseudouridine synthases showed very different substrate selectivity. While TruB1 selectively and specifically interacts with pri-let-7 and promotes let-7 expression, PUS10 appears to non-specifically increase maturation of various miRNAs (Song *et al*, 2019). Consistent with this, our endogenous HITS-CLIP for TruB1, and the published PUS10 PAR-CLIP analysis, reveal that TruB1 binds to the terminal loop of let-7, while PUS10 binds to a site relatively far from the terminal loop of miRNAs (Song *et al*, 2019). Furthermore, TruB1 acts suppressively on cell proliferation due to the selective promotion of let-7 maturation, whereas PUS10 tended to promote cell proliferation (Song *et al*, 2019). Thus, TruB1 functions differently to PUS10.

TruB is known to be an RNA-modifying enzyme that possesses two distinct molecular functions: RNA folding and subsequent RNA

modification. There are other such examples of RBPs with dual functions in addition to their intrinsic enzymatic activity (i.e., ADAR1/2, METTL3, METTL16) (Ota *et al*, 2013; Lin *et al*, 2016; Pendleton *et al*, 2017). Our strategy and data reveal an unexpected function of TruB1 in miRNAs biogenesis with let-7 specificity and present a new aspect of miRNA regulation by RNA-binding proteins.

Materials and Methods

Plasmid construction

The pLuc2-KAP-MCS vector was generated by a previously reported method (Ito *et al*, 2017). To create the let-7 sensor vector, the chemically synthesized let-7 complementary sequence was annealed and inserted between the EcoRI and XhoI sites. We used the empty pLus2-KAP-MCS vector as the control sensor (−) vector. The KRAS mRNA vector was generated by inserting the let-7a target site of Kras mRNA into pLuc2-KAP-MCS at the EcoR1 and Kpn1 sites. The sequence encoding human TruB1 ORF was cloned by PCR from 293FT cell cDNA. pcDNA-TruB1 was generated by inserting the ORF of human TruB1 with a Flag sequence into pcDNA.3.1(+) (Thermo Fisher Scientific) at the Nhe1 and EcoR1 sites. The pCLT vector was designed and created by modifying pCS 2 (RIKEN) using the tet-on system. The sequence is shown in Table EV5. pCLT-TruB1 and pCLT-GFP were generated by inserting the ORF of human TruB1 and GFP with a Flag sequence into the pCLT vector at the Nhe1 and EcoR1 sites. pCLT-mt1 and mt2 were generated by PrimeSTAR Mutagenesis Basal Kit (Takara). pET22b-TruB1, mt1, and mt2 were generated by inserting the ORF of human TruB1 and its mutants into the pET22b vector (Merck Millipore) at the NdeI and XhoI sites. pcDNA-pri-let-7a1 was generated by inserting the human pri-let-7a1 sequence into pcDNA.3.1(+) at the BamH1 and Not1 sites. Loop mt was generated by inverse PCR from pcDNA-pri-let-7a1. The nucleotide sequences of the primers used for the PCR are shown in Table EV4.

Cell culture

HEK293FT, A549, and HeLa cells were maintained in DMEM (Corning) supplemented with 10% FBS (Gibco) and 1% penicillin–streptomycin (Wako) at 37°C with 5% CO_2. siRNAs [(TruB1 (NM_139169.3), TruB2 (NM_015679.1), Dicer1 (23405-1-B and 23405-2-B) or negative controls (SN-1002); Bioneer), (LIN28B (s52477) or negative control (AM4611); Ambion, Life Technologies) and 2′-O-methylated antisense inhibitor (let-7 family or negative control: detailed sequences shown in Table EV4, Nippon-shinyaku)] were transfected into cells using Lipofectamine RNAiMAX (Thermo Fisher Scientific) using the manufacturer's recommended protocol. For transient overexpression, pcDNA vectors (pcDNA-TruB1-Flag) were transfected with FuGENE HD (Promega) into cells according to the manufacturer's instructions. For steady-state expression, lentiviral vectors [pCLT vectors (pCLT-GFP, TruB1, and its mutants)] were used with doxycycline (Clontech) treatment (1.0 μg/ml) for 5 days. For virus production, HEK293FT cells were transfected with the lentiviral vector pCLTs together with the packaging plasmids pCMV-VSVG-RSV-Rev (addgene) and pCAG-HIVgp (addgene) at a 1:0.5:0.5 ratio using PEI-Max reagent (Polysciences) according to the

manufacturer's instructions. Supernatants were harvested 48 h after transfection. Cells (5×10^5) were mixed in 2 ml viral supernatant supplemented with 8 μg/ml polybrene (Merck Millipore) and further incubated at 37°C. The infected cells were selected by 1 μg/ml puromycin (Thermo Fisher Scientific) and kept in selection medium for 7 days.

Genome editing

TruB1-Flag-tagged HEK-293FT cells were established by using CRISPR–Cas9 system. ALT-R XT CRISPR RNA (crRNA) (Integrated DNA Technologies) and ALT-R trans-activating crRNA (tracrRNA) (Integrated DNA Technologies) were resuspended in Nuclease-free-duplex buffer (Integrated DNA Technologies) to a final concentration of 100 μM. crRNA and tracRNA with equal volumes were mixed and heated for 5 min at 95°C, followed by gradually cooling down to room temperature. Mixed RNAs were incubated at room temperature for 20 min with ALT-R Cas9 Nuclease V3 (61 μM) (Integrated DNA Technologies) and single-stranded oligo DNA (ssODN) including sequences of HiBIT, 3 x Flag and complementary sequence of N-terminal in TruB1 genome. Next, this RNA, protein, and ssODN were co-transfected into HEK-293FT cells using a NEPA21 Super Electroporator (NEPAGENE). We used the HiBIT system to detect the knocked-in cells (Schwinn *et al*, 2018) with dilution methods. After transfection, knocked-in cells were detected by Nano Glo HiBiT Lytic Detection System (Promega) using the manufacturer's recommended protocol. Knocked-in cells were verified by PCR and Western blotting with anti-Flag antibody (MBL).

Cell-based screening

We created 384-well reporter library plates for cell-based screening. In detail, library plasmids were diluted to 4 ng/μl in elution buffer (10 mM Tris–HCl; pH 8.5) in 96-well plates and were then dispensed into 384-well culture plates at 5 μl per well. Cell-based screening for let-7 regulator genes was performed by modifying a previously described method (Ito *et al*, 2017). Five microliters of OPTI-MEM (Gibco) containing 0.15 μl of PEI-Max (Polyscience), 20 ng of sensor vector or control sensor (−) vector, and 5 ng of pRL-SV40 (Promega) Renilla luciferase construct was added to the 384-well reporter library plates and incubated for 20 min. Then, 293FT cells (Thermo Fisher Scientific) in 40 μl of DMEM containing 10% of FBS were added into each well using an automated multidispenser ECO DROPPER III (AS ONE). The cells were cultured in a 5% CO_2 incubator at 37°C for 48 h. Luciferase activity was measured by means of an ARVO X3 (PerkinElmer) and the Dual-Glo Luciferase Assay System (Promega).

Luciferase reporter assay

Luciferase assays were performed by incubating 20 μl of OPTI-MEM containing 0.4 μl of FuGENE HD, 25 ng of reporter plasmids and 5 ng of pRL-SV40 for 10 min in 96-well culture plates. Then, 293FT cells in 100 μl of DMEM containing 10% of FBS were added to each well and cultured for 48 h. Luciferase activity was measured using an ARVO X3 (PerkinElmer) and the Dual-Glo Luciferase Assay System (Promega).

Reverse transcription and RT–qPCR

Total RNA samples were extracted using ISOGEN (NIPPON GENE). To evaluate mRNA expression, reverse transcription was carried out using oligo dT primers (Thermo Fisher Scientific) and SuperScript III (Thermo Fisher Scientific). Quantitative RT–PCR (qRT–PCR) was run using THUNDERBIRD SYBR qPCR Mix (TOYOBO). The results are expressed as mRNA levels normalized to GAPDH mRNA expression in each sample. To evaluate microRNA expression, reverse transcription was performed using the TaqMan MicroRNA Reverse Transcription Kit (Thermo Fisher Scientific) and TaqMan MicroRNA Assays (Thermo Fisher Scientific). Quantitative RT–PCR (qRT–PCR) was run using THUNDERBIRD Probe qPCR Mix (TOYOBO). The results are expressed as RNA levels normalized to RNU6B expression in each sample. The primer sequences and assays used for the real-time PCR are listed in Table EV4. To determine RNA levels, at least three independent RNA samples were analyzed.

Northern blotting

LNA/DNA probes (PAGE grade, fasmac, Table EV4) were labeled with 32P-γ-ATP by means T4PNK (Takara), followed to filter by MicroSpin G-25 Columns (GE healthcare). 4 μg of small RNA purified by the mirVana miRNA Isolation kit (Thermo Fisher Scientific) was heated at 90°C for 20 s with gel loading buffer II (Thermo Fisher Scientific) and placed on ice, followed by running on a 10% TBE-Urea PAGE. RNA was transferred to a Hybond-N+ membrane (GE Healthcare) at 4 mA/cm^2 for 45 min and fixed by UV-cross-linking. The membrane was dried and pre-hybridized at 37°C for 30 min in ExpressHyb (Clontech). Hybridization was performed in ExpressHyb containing RI-labeled probe at 37°C overnight with rotation. Subsequently, the membrane was washed twice in low stringency buffer (2× SSC, 0.05% SDS) at room temperature for 30 min and twice in high stringency buffer (0.5× SSC, 0.1% SDS) at room temperature for 40 min. Membranes were exposed to an autoradiography film. Decade Markers System (to make radiolabeled RNA markers) (Thermo Fisher Scientific) was used as a size marker.

TaqMan array

Total RNA was isolated using the mirVana miRNA isolation kit (Thermo Fisher Scientific). 3 μl of RNA (1,000 ng) was reverse-transcribed by Megaplex RT Primers, Pool A (human) (Thermo Fisher Scientific) using the TaqMan® microRNA Reverse Transcription Kit (Thermo Fisher Scientific). For qRT–PCR, RT product was mixed with TaqMan® Universal PCR Master Mix, No AmpErase UNG (Thermo Fisher Scientific) and the appropriate amount of water, and subsequently loaded into the ports of the TaqMan array cards. Real-Time PCR was performed on a 7900HT Fast Real-Time PCR System with TaqMan® Array Block (Thermo Fisher Scientific), using universal cycling conditions [95°C/10 min, then (95°C/15 s, 60°C/60 s) for 40 cycles]. Raw Ct values were normalized to RNU6B.

Western blotting

Total protein samples were extracted by radioimmunoprecipitation assay (RIPA) buffer [50 mM Tris–HCl (pH 8.0), 150 mM NaCl, 0.5% deoxycholate (DOC), 0.1% SDS, 1% Nonidet P-40]. Proteins in the cell lysates were separated by SDS/PAGE followed by semidry transfer to a PVDF membrane. Membranes were blocked for 60 min with Blocking One (Nacalai Tesque), incubated with an anti-Flag (M185-3L, MBL), anti-DGCR8 (ab90579, Abcam), anti-Lin28B (11965S, Cell signaling technologies), anti-KRAS (ab180772, Abcam), or anti-β-actin (A5316; Sigma Aldrich) at 4°C overnight, rinsed, and then incubated for 1 h with ECL mouse IgG HRP-conjugated whole antibody (GE Healthcare) or rabbit IgG HRP-conjugated whole antibody (GE Healthcare). The blot was developed with the ECL Select Western Blotting Detection Reagent (GE Healthcare). The protein levels are normalized to β-actin levels in each sample.

HITS-CLIP

Flag-tagged cells were collected and crosslinked with 254 nm UV-crosslinking at 400 and 200 mJ/cm^2 on ice in a Ultraviolet Cross-linker (UVP). The cells were collected, centrifuged, and resuspended in Lysis buffer (1× PBS, 0.1% SDS, 0.5% DOC, 0.5% NP-40). After incubation with rotation for 10 min at 4°C, cells were sonicated 30 s/30 s (on/off) for 5 cycles by Bioruptor (Cosmo BIO). Then, whole cell lysate was collected by centrifugation at 13,000 g for 15 min at 4°C and treated with 5 U/ml RNase T1 (Thermo Fisher Scientific) and Turbo DNase (Thermo Fisher Scientific) for 5 min at 37°C. Three different doses of RNaseT1 and one non-crosslinked cells were used as controls. For immunoprecipitation, we used mouse anti-FLAG antibody (MBL) and normal mouse IgG (Sigma Aldrich) as an additional negative control. Antibodies were coupled to Dynabeads Protein G (Thermo Fisher Scientific) following the manufacturer's protocol. Coupled antibodies were washed with PBST. RNaseT1-treated whole cell lysate and coupled antibodies were mixed and rotated at 4°C for 2 h. Antibody-bound proteins and RNA-protein complexes were isolated by magnetic stand and washed with wash buffer (1× PBS, 0.1% SDS, 0.5% DOC, 0.5% NP-40) and high-salt-wash buffer (5× PBS, 0.1% SDS, 0.5% DOC, 0.5% NP-40). Purified RNA fragments were treated with CIP (Takara) and ligated with 3′ linker adaptor by using T4 RNA ligase (Thermo Fisher Scientific) at 16°C overnight. Treated RNA fragments were labeled with 32p-γ-ATP, followed by electrophoresis with SDS–PAGE (NuPAGE, Thermo Fisher Scientific) and transferred to nitro-cellulose membranes. RI-labeled RNAs were detected by autoradiography. Appropriate bands or smear-bands were picked up from the membrane and treated with Proteinase K (Roche). RNA fragments were purified by Acid phenol:CHCL$_3$ (Thermo Fisher Scientific). Purified TruB1-bound RNA fragments were ligated with 5′ linker RNA, followed by the reverse-transcriptase reaction using RT primers and SuperScript III (Thermo Fisher Scientific). cDNA libraries were amplified by means of Phusion High-Fidelity DNA Polymerase (New England Biolabs). Quantification of libraries was calculated using Quibit3.0 (Thermo Fisher Scientific), TapeStation (Agilent) with High Sensitivity DNA Kit, and qPCR analysis by NEB Next Library Quant Kit for Illumina (New England Biolabs). All sequencing was performed using an Illumina MiSeq (Illumina) with MiSeq Reagent Kit v3 (Illumina).

HITS-CLIP analysis

Raw reads (fastq file) obtained from the Illumina pipeline were checked, trimmed, and clipped using Bioconductor, FastQC, FASTX-

toolkit, and cutadapt (v.1.2.1) (Martin, 2011) and were subsequently mapped to the human genome (build hg38) using bowtie2 (Langmead & Salzberg, 2012). To eliminate reads in which the adaptor was ligated more than once, adaptor removal was performed three times. Duplicate reads were filtered by IGV tools (Robinson et al, 2011). All data analysis was done using a combination of custom and publicly available tools (featureCounts (Liao et al, 2014), SAMtools (Li et al, 2009), RSeQC (Wang et al, 2012), bedtools (Quinlan & Hall, 2010), tRNAscan-SE 2.0 (Lowe & Chan, 2016) and R) including resources available from the UCSC Genome Browser and Galaxy Bioinformatics (http://main.g2.bx.psu.edu/). All aligned reads shorter than 10 nt that mapped to more than a single position in the genome were excluded from further analysis. In trimmed data, the 500-bp flanking sequences of known pre-miRNAs were extracted as pri-miRNAs. Transcript annotation was acquired from UCSC. The read count is plotted for miRNAs with TaqMan array data in this report. Data were normalized by expression levels of each microRNA in control samples of the TaqMan array.

Motif analysis

We identified motifs for sequences mapped to tRNAs. Reads were randomly selected within 5,000 reads by seqkit (https://bioinf.she nwei.me/seqkit/) (Shen et al, 2016) to perform the following analysis. Multiple Em for Motif Elicitation (MEME) was performed using v.4.9.1 of the MEME browser application (Bailey et al, 2009).

RNA immunoprecipitation (RIP)

Cells were collected, centrifuged, and resuspended in Lysis buffer (1× PBS, 0.1% SDS, 0.5% DOC, 0.5% NP-40). After incubation with rotation for 10 min at 4°C, cells were sonicated 30 s/30 s (on/off) for five cycles. Then, whole cell lysate was collected by centrifugation at 13,000 g for 15 min at 4°C. For immunoprecipitation, we used mouse anti-FLAG (MBL), anti-DGCR8 (Abcam), and normal mouse IgG (Sigma Aldrich) as an additional negative control. Antibodies were coupled to Protein G Dynabeads (Thermo Fisher Scientific) following the manufacturer's protocol. Coupled antibodies were washed with PBST. Whole cell lysate and coupled antibodies were mixed and rotated at 4°C for 2 h. Antibody-bound proteins and RNA-protein complex were isolated by magnetic stand and washed with wash buffer (1× PBS, 0.1% SDS, 0.5% DOC, 0.5% NP-40) and high-salt-wash buffer (5× PBS, 0.1% SDS, 0.5% DOC, 0.5% NP-40). RNA was eluted by Acid phenol:CHCL$_3$ (Thermo Fisher Scientific). Pri-miRNA levels were analyzed by qRT–PCR. Relative ratio of protein bound pri-miRNA was calculated as compared to its input sample.

Immunoprecipitation

Cells were collected, centrifuged, and resuspended in Lysis buffer (25 mM Tris–HCl (pH 7.4), 150 mM NaCl, 1 mM EDTA, 1% NP-40, 5% glycerol). After incubation with rotation for 10 min at 4°C, cells were sonicated 30 s/30 s (on/off) for five cycles. Then, whole cell lysate was collected by centrifugation at 13,000 g for 15 min at 4°C. For immunoprecipitation, we used mouse anti-FLAG (MBL), anti-DGCR8 (Abcam), and normal mouse IgG (Sigma Aldrich) as

an additional negative control. Antibodies were coupled to Protein G Dynabeads (Thermo Fisher Scientific) following the manufacturer's protocol. Coupled antibodies were washed with PBST. Whole cell lysate and coupled antibodies were mixed and rotated at 4°C for 2 h. Antibody-bound proteins and protein complex were isolated by magnetic stand and washed with Lysis buffer. Proteins in the lysates were separated by SDS/PAGE followed by semidry transfer to a PVDF membrane as described in Western blotting. Membranes were blocked for 60 min with Blocking One (Nacalai Tesque), incubated with an anti-Flag (M185-3L, MBL), anti-DGCR8 (ab90579, Abcam), or anti-β-actin (A5316; Sigma Aldrich) at 4°C overnight, rinsed, and then incubated for 1 h with Clean Blot IP Detection Reagent (HRP) (Thermo Fisher Scientific). The blot was developed with the ECL Select Western Blotting Detection Reagent (GE Healthcare).

In vitro processing assay

pri-miRNAs were *in vitro* transcribed using MEGA script T7 Transcription Kit (Thermo Fisher Scientific) with a 32p-α-UTP (RI) label, followed by PAGE purification. We also synthesized RI-labeled pri-let-7a1 in which pseudouridine was randomly introduced using UTP: pseudouridine (Carbosynth) at a ratio of 1:1. Cells were collected, centrifuged, and resuspended in 200 μl of Lysis buffer (WCL) (20 mM Tris–HCl (pH 8.0), 100 mM KCl, 0.5 mM EDTA, 5% glycerol, 0.5 mM PMSF, and 5 mM DTT). After incubation with rotation for 10 min at 4°C, cells were sonicated 15 s/90 s (on/off) for three cycles. Whole cell lysate was collected by centrifugation at 18,000 g for 15 min at 4°C. Labeled RNA was treated with whole cell lysate and 6.4 mM MgCl$_2$ at 37°C for 90 min. RNA was eluted by Acid phenol:CHCL$_3$ (Thermo Fisher Scientific) and run on 10% TBE-Urea PAGE. RNA was visualized by autoradiography after gel drying. Decade Markers System (to make radiolabeled RNA markers) (Thermo Fisher Scientific) was used as a size marker.

Electrophoretic mobility shift assay (EMSA)

pri-miRNAs were *in vitro* transcribed using MEGA script T7 Transcription Kit (Thermo Fisher Scientific) with 32p-α-UTP to label by RI, followed by PAGE purification. Labeled RNA and recombinant proteins were mixed and incubated at 37°C for 1 h, followed by naïve PAGE. RNA and RNA–protein complexes were visualized by autoradiography.

Expression and purification of recombinant proteins

Escherichia coli BL21 (DE3) (Novagen) was transformed by the plasmids, and the transformants were grown at 37°C until the A600 reached 1.0. The expression of the TruB1 proteins was induced by adding isopropyl-β-D thiogalactopyranoside at a final concentration of 0.1 mM and incubating the cultures for 18 h at 18°C. The cells were collected and lysed by sonication in buffer, containing 20 mM Tris–HCl, pH 7.0, 500 mM NaCl, 10 mM β-mercaptoethanol, 20 mM imidazole, 0.1 mM phenylmethylsulfonyl fluoride, and 5% (v/v) glycerol. The proteins were first purified by chromatography on a Ni-NTA agarose column (QIAGEN) and then further purified on a HiTrap Heparin column (GE Healthcare). Finally, the proteins were purified by chromatography on a HiLoad 16/60 Superdex 200

column (GE Healthcare), in buffer containing 20 mM Tris–HCl, pH 7.0, 200 mM NaCl, and 10 mM β-mercaptoethanol. The purified proteins were concentrated and stored at −80°C until use. The hTruB1 mutants were purified in a similar manner.

In vitro enzymatic activity assay

pri-miRNAs were *in vitro* transcribed using MEGA script T7 Transcription Kit (Thermo Fisher Scientific) with 32p-α-UTP, followed by PAGE purification. Labeled RNA was treated with recombinant TruB1 or its mutants in reaction buffer (20 mM Tris–HCl (pH 8.0), 0.1 mM EDTA, 100 mM NaCl, 5 mM DTT and 100 mM NH_4Cl) at 37°C for 60 min. RNA was eluted by Acid phenol:CHCL$_3$ (Thermo Fisher Scientific) and treated with Nuclease P1 (New England BioLab) at 37°C for 3 h. RNA was run on 1D-thin layer chromatography on cellulose plates (TLC, 20 cm, Merck Millipore) with solvent (isopropanol/HCl/water (70/15/15); $v/v/v$) for 6 h at room temperature. RNA was visualized by autoradiography.

CMC primer extension assay

Primers (PAGE grade, fasmac, Table EV4) were labeled with 32P-γ-ATP by T4PNK (Takara), followed by filtering through MicroSpin G-25 Columns (GE healthcare). 4 μg of total RNA was treated with 0.17 M N-cyclohexyl-N0-(2-morpholinoethyl)carbodiimide metho-p-toluenesulfonate (CMC, Tokyo Kasei) in reaction buffer (7 M urea, 50 mM Bicine and 4 mM EDTA) at 37°C for 20 min. Reaction was stopped with 100 μl of stop buffer [0.3 M NaOAc and 0.1 mM EDTA, pH 5.6] and 700 μl of EtOH. After incubation at −80°C for 1 h, the treated RNA was centrifuged, and washed twice with 70% EtOH. RNA pellet was dissolved in 50 mM Na_2CO_3 (pH 10.4) and incubated at 37°C for 4 h. Reaction was stopped in the same manner. RNA pellet was dissolved in water and purified using the RNeasy MinElute Cleanup kit (QIAGEN). Treated RNA was reverse-transcribed with RI-labeled primer by SuperScript III (Thermo Fisher Scientific) with or without ddATP solution (Thermo Fisher Scientific). cDNA was eluted by phenol/chloroform/isoamyl alcohol (Thermo Fisher Scientific) and run on 10% TBE-Urea PAGE. cDNA was visualized by autoradiography after gel drying. Synthesized RNA (Fasmac) was used as a size marker (20nt, 25nt and 35nt).

Evaluation of cell viability

Cell viability was determined using Real-Time-Glo MT Cell Viability Assay (Promega). A total of 1,000 cells/well were plated in 96-well culture plates. After 24 h of incubation, the medium was changed to a growth medium with MT Cell Viability Substrate (Promega) and Nano Luc Enzyme (Promega). Then, the cells were incubated for an additional 0, 12, 24, 48, 72 h of culture. The luminescence in the resulting solution was measured using an ARVO X3 (PerkinElmer) at each point. Cell viability was determined by dividing the luminescence activity by that of the control cells. These experiments were conducted on at least three independent samples.

Data analysis from public databases

We browsed several series (GEO accession GSE3325, GDS4102, GSE64333_at; Data ref: Varambally *et al*, 2005b; Data ref: Pei *et al*, 2009b; Data ref: Wang *et al*, 2015b) of the GEO Profiles database (Edgar *et al*, 2002).

Quantification and statistical analysis

Blot signals were quantified using ImageJ (NIH) (Schneider *et al*, 2012). Data are presented as the means ± standard errors, and differences between groups were evaluated using the two-tailed Student's *t*-test. A *P*-value of < 0.05 was considered statistically significant. Asterisk in figures indicate differences with statistical significance as follows: *$P < 0.05$. All the experiments were conducted in close adherence to the institutional regulations.

Data availability

The datasets produced in this study are available in the following databases:

- The raw data of TaqMan array: Gene Expression, Omnibus GSE143510 (https://www.ncbi.nlm.nih.gov/geo/query/acc.cgi?&acc = GSE143508)
- The raw data of HITS-CLIP: Other (HITS-CLIP), Omnibus GSE143510 (https://www.ncbi.nlm.nih.gov/geo/query/acc.cgi?acc = GSE143510) All the other data required to reproduce this study are included in this published article and supplementary information. All reagents and materials used in this study are available in Appendix. Further information and requests for resources and reagents should be directed to and will be fulfilled by Hiroshi Asahara (asahara@scripps.edu or asahara.syst@tmd.ac.jp).

Expanded View for this article is available online.

Author contributions
RK, TC, YI, TM, KM, TS, KT, and HA designed the study; RK performed experiments, analyzed data; KT created and purified recombinant proteins; RK, TC, and YYan generated sequencing data. YYas prepared the cellular material; TS and KT supervised the project; RK, TS, KT, and HA drafted the manuscript; HA critically reviewed the manuscript; and all authors approved the final manuscript.

Conflict of interest
The authors declare that they have no conflict of interest.

References

Ambros V (2004) The functions of animal microRNAs. *Nature* 431: 350 – 355

Antonicka H, Choquet K, Lin ZY, Gingras AC, Kleinman CL, Shoubridge EA (2017) A pseudouridine synthase module is essential for mitochondrial protein synthesis and cell viability. *EMBO Rep* 18: 28 – 38

Arroyo JD, Jourdain AA, Calvo SE, Ballarano CA, Doench JG, Root DE, Mootha VK (2016) A genome-wide CRISPR death screen identifies genes essential for oxidative phosphorylation. *Cell Metab* 24: 875 – 885

Auyeung VC, Ulitsky I, McGeary SE, Bartel DP (2013) Beyond secondary structure: primary-sequence determinants license pri-miRNA hairpins for processing. *Cell* 152: 844 – 858

Bailey TL, Boden M, Buske FA, Frith M, Grant CE, Clementi L, Ren J, Li WW, Noble WS (2009) MEME SUITE: tools for motif discovery and searching. *Nucleic Acids Res* 37: W202 – W208

Bartel DP (2018) Metazoan microRNAs. *Cell* 173: 20 – 51

Becker HF, Motorin Y, Planta RJ, Grosjean H (1997) The yeast gene YNL292w encodes a pseudouridine synthase (Pus4) catalyzing the formation of psi55 in both mitochondrial and cytoplasmic tRNAs. *Nucleic Acids Res* 25: 4493 – 4499

Bohnsack MT, Czaplinski K, Gorlich D (2004) Exportin 5 is a RanGTP-dependent dsRNA-binding protein that mediates nuclear export of pre-miRNAs. *RNA* 10: 185 – 191

Cai X, Hagedorn CH, Cullen BR (2004) Human microRNAs are processed from capped, polyadenylated transcripts that can also function as mRNAs. *RNA* 10: 1957 – 1966

Carlile TM, Rojas-Duran MF, Zinshteyn B, Shin H, Bartoli KM, Gilbert WV (2014) Pseudouridine profiling reveals regulated mRNA pseudouridylation in yeast and human cells. *Nature* 515: 143 – 146

Chanda SK, White S, Orth AP, Reisdorph R, Miraglia L, Thomas RS, DeJesus P, Mason DE, Huang Q, Vega R *et al* (2003) Genome-scale functional profiling of the mammalian AP-1 signaling pathway. *Proc Natl Acad Sci USA* 100: 12153 – 12158

Chang TC, Zeitels LR, Hwang HW, Chivukula RR, Wentzel EA, Dews M, Jung J, Gao P, Dang CV, Beer MA *et al* (2009) Lin-28B transactivation is necessary for Myc-mediated let-7 repression and proliferation. *Proc Natl Acad Sci USA* 106: 3384 – 3389

Charette M, Gray MW (2000) Pseudouridine in RNA: what, where, how, and why. *IUBMB Life* 49: 341 – 351

Chendrimada TP, Gregory RI, Kumaraswamy E, Norman J, Cooch N, Nishikura K, Shiekhattar R (2005) TRBP recruits the Dicer complex to Ago2 for microRNA processing and gene silencing. *Nature* 436: 740 – 744

Choudhury NR, Nowak JS, Zuo J, Rappsilber J, Spoel SH, Michlewski G (2014) Trim25 is an RNA-specific activator of Lin28a/TuT4-mediated uridylation. *Cell Rep* 9: 1265 – 1272

Cohn WE, Volkin E (1951) Nucleoside-5′-phosphates from ribonucleic acid. *Nature* 167: 483 – 484

Conkright MD, Canettieri G, Screaton R, Guzman E, Miraglia L, Hogenesch JB, Montminy M (2003) TORCs: transducers of regulated CREB activity. *Mol Cell* 12: 413 – 423

Denli AM, Tops BB, Plasterk RH, Ketting RF, Hannon GJ (2004) Processing of primary microRNAs by the microprocessor complex. *Nature* 432: 231 – 235

Deogharia M, Mukhopadhyay S, Joardar A, Gupta R (2019) The human ortholog of archaeal Pus10 produces pseudouridine 54 in select tRNAs where its recognition sequence contains a modified residue. *RNA* 25: 336 – 351

Edgar R, Domrachev M, Lash AE (2002) Gene Expression Omnibus: NCBI gene expression and hybridization array data repository. *Nucleic Acids Res* 30: 207 – 210

Friedt J, Leavens FM, Mercier E, Wieden HJ, Kothe U (2014) An arginine-aspartate network in the active site of bacterial TruB is critical for catalyzing pseudouridine formation. *Nucleic Acids Res* 42: 3857 – 3870

Gregory RI, Yan KP, Amuthan G, Chendrimada T, Doratotaj B, Cooch N, Shiekhattar R (2004) The microprocessor complex mediates the genesis of microRNAs. *Nature* 432: 235 – 240

Grishok A, Pasquinelli AE, Conte D, Li N, Parrish S, Ha I, Baillie DL, Fire A, Ruvkun G, Mello CC (2001) Genes and mechanisms related to RNA interference regulate expression of the small temporal RNAs that control *C. elegans* developmental timing. *Cell* 106: 23 – 34

Gutgsell N, Englund N, Niu L, Kaya Y, Lane BG, Ofengand J (2000) Deletion of the *Escherichia coli* pseudouridine synthase gene truB blocks formation of pseudouridine 55 in tRNA *in vivo*, does not affect exponential growth, but confers a strong selective disadvantage in competition with wild-type cells. *RNA* 6: 1870 – 1881

Ha M, Kim VN (2014) Regulation of microRNA biogenesis. *Nat Rev Mol Cell Biol* 15: 509 – 524

Han J, Lee Y, Yeom KH, Kim YK, Jin H, Kim VN (2004) The Drosha-DGCR8 complex in primary microRNA processing. *Genes Dev* 18: 3016 – 3027

Heo I, Joo C, Cho J, Ha M, Han J, Kim VN (2008) Lin28 mediates the terminal uridylation of let-7 precursor MicroRNA. *Mol Cell* 32: 276 – 284

Hoang C, Ferre-D'Amare AR (2001) Cocrystal structure of a tRNA Psi55 pseudouridine synthase: nucleotide flipping by an RNA-modifying enzyme. *Cell* 107: 929 – 939

Huang Q, Raya A, DeJesus P, Chao SH, Quon KC, Caldwell JS, Chanda SK, Izpisua-Belmonte JC, Schultz PG (2004) Identification of p53 regulators by genome-wide functional analysis. *Proc Natl Acad Sci USA* 101: 3456 – 3461

Hutvágner G, McLachlan J, Pasquinelli AE, Balint E, Tuschl T, Zamore PD (2001) A cellular function for the RNA-interference enzyme Dicer in the maturation of the let-7 small temporal RNA. *Science* 293: 834 – 838

Iourgenko V, Zhang W, Mickanin C, Daly I, Jiang C, Hexham JM, Orth AP, Miraglia L, Meltzer J, Garza D *et al* (2003) Identification of a family of cAMP response element-binding protein coactivators by genome-scale functional analysis in mammalian cells. *Proc Natl Acad Sci USA* 100: 12147 – 12152

Ito Y, Inoue A, Seers T, Hato Y, Igarashi A, Toyama T, Taganov KD, Boldin MP, Asahara H (2017) Identification of targets of tumor suppressor microRNA-34a using a reporter library system. *Proc Natl Acad Sci USA* 114: 3927 – 3932

Johnson SM, Grosshans H, Shingara J, Byrom M, Jarvis R, Cheng A, Labourier E, Reinert KL, Brown D, Slack FJ (2005) RAS is regulated by the let-7 microRNA family. *Cell* 120: 635 – 647

Keffer-Wilkes LC, Veerareddygari GR, Kothe U (2016) RNA modification enzyme TruB is a tRNA chaperone. *Proc Natl Acad Sci USA* 113: 14306 – 14311

Ketting RF, Fischer SE, Bernstein E, Sijen T, Hannon GJ, Plasterk RH (2001) Dicer functions in RNA interference and in synthesis of small RNA involved in developmental timing in *C. elegans*. *Genes Dev* 15: 2654 – 2659

Knight SW, Bass BL (2001) A role for the RNase III enzyme DCR-1 in RNA interference and germ line development in *Caenorhabditis elegans*. *Science* 293: 2269 – 2271

Krol J, Loedige I, Filipowicz W (2010) The widespread regulation of microRNA biogenesis, function and decay. *Nat Rev Genet* 11: 597 – 610

Landthaler M, Yalcin A, Tuschl T (2004) The human DiGeorge syndrome critical region gene 8 and its *D. melanogaster* homolog are required for miRNA biogenesis. *Curr Biol* 14: 2162 – 2167

Langmead B, Salzberg SL (2012) Fast gapped-read alignment with Bowtie 2. *Nat Methods* 9: 357–359

Lee RC, Feinbaum RL, Ambros V (1993) The *C. elegans* heterochronic gene lin-4 encodes small RNAs with antisense complementarity to lin-14. *Cell* 75: 843–854

Lee Y, Ahn C, Han J, Choi H, Kim J, Yim J, Lee J, Provost P, Radmark O, Kim S *et al* (2003) The nuclear RNase III Drosha initiates microRNA processing. *Nature* 425: 415–419

Lee Y, Kim M, Han J, Yeom KH, Lee S, Baek SH, Kim VN (2004) MicroRNA genes are transcribed by RNA polymerase II. *EMBO J* 23: 4051–4060

Lee Y, Hur I, Park SY, Kim YK, Suh MR, Kim VN (2006) The role of PACT in the RNA silencing pathway. *EMBO J* 25: 522–532

Li H, Handsaker B, Wysoker A, Fennell T, Ruan J, Homer N, Marth G, Abecasis G, Durbin R, Genome Project Data Processing S (2009) The sequence Alignment/Map format and SAMtools. *Bioinformatics* 25: 2078–2079

Li X, Zhu P, Ma S, Song J, Bai J, Sun F, Yi C (2015) Chemical pulldown reveals dynamic pseudouridylation of the mammalian transcriptome. *Nat Chem Biol* 11: 592–597

Liao Y, Smyth GK, Shi W (2014) featureCounts: an efficient general purpose program for assigning sequence reads to genomic features. *Bioinformatics* 30: 923–930

Lin S, Choe J, Du P, Triboulet R, Gregory RI (2016) The m(6)A methyltransferase METTL3 promotes translation in human cancer cells. *Mol Cell* 62: 335–345

Liu J, Bang AG, Kintner C, Orth AP, Chanda SK, Ding S, Schultz PG (2005) Identification of the Wnt signaling activator leucine-rich repeat in flightless interaction protein 2 by a genome-wide functional analysis. *Proc Natl Acad Sci USA* 102: 1927–1932

Liu Z, Wang J, Cheng H, Ke X, Sun L, Zhang QC, Wang HW (2018) Cryo-EM structure of human Dicer and its complexes with a pre-miRNA substrate. *Cell* 173: 1191–1203

Lowe TM, Chan PP (2016) tRNAscan-SE On-line: integrating search and context for analysis of transfer RNA genes. *Nucleic Acids Res* 44: W54–W57

Lund E, Guttinger S, Calado A, Dahlberg JE, Kutay U (2004) Nuclear export of microRNA precursors. *Science* 303: 95–98

Martin M (2011) Cutadapt removes adapter sequences from high-throughput sequencing reads. *EMBnetjournal* 17: 10–12

Michlewski G, Guil S, Semple CA, Cáceres JF (2008) Posttranscriptional regulation of miRNAs harboring conserved terminal loops. *Mol Cell* 32: 383–393

Michlewski G, Caceres JF (2010) Antagonistic role of hnRNP A1 and KSRP in the regulation of let-7a biogenesis. *Nat Struct Mol Biol* 17: 1011–1018

Mourelatos Z, Dostie J, Paushkin S, Sharma A, Charroux B, Abel L, Rappsilber J, Mann M, Dreyfuss G (2002) miRNPs: a novel class of ribonucleoproteins containing numerous microRNAs. *Genes Dev* 16: 720–728

Newman MA, Thomson JM, Hammond SM (2008) Lin-28 interaction with the Let-7 precursor loop mediates regulated microRNA processing. *RNA* 14: 1539–1549

Ota H, Sakurai M, Gupta R, Valente L, Wulff BE, Ariyoshi K, Iizasa H, Davuluri RV, Nishikura K (2013) ADAR1 forms a complex with Dicer to promote microRNA processing and RNA-induced gene silencing. *Cell* 153: 575–589

Pandolfini L, Barbieri I, Bannister AJ, Hendrick A, Andrews B, Webster N, Murat P, Mach P, Brandi R, Robson SC *et al* (2019) METTL1 promotes let-7 microRNA processing via m7G methylation. *Mol Cell* 74: 1278–1290

Pei H, Li L, Fridley BL, Jenkins GD, Kalari KR, Lingle W, Petersen G, Lou Z, Wang L (2009a) FKBP51 affects cancer cell response to chemotherapy by negatively regulating Akt. *Cancer Cell* 16: 259–266

Pei H, Li L, Fridley BL, Jenkins GD, Kalari KR, Lingle W, Petersen G, Lou Z, Wang L (2009b) Gene Expression Omnibus GDS4102 (https://www.ncbi.nlm.nih.gov/sites/GDSbrowser?acc=GDS4102). [DATASET]

Pendleton KE, Chen B, Liu K, Hunter OV, Xie Y, Tu BP, Conrad NK (2017) The U6 snRNA m(6)A methyltransferase METTL16 regulates SAM synthetase intron retention. *Cell* 169: 824–835

Piskounova E, Viswanathan SR, Janas M, LaPierre RJ, Daley GQ, Sliz P, Gregory RI (2008) Determinants of microRNA processing inhibition by the developmentally regulated RNA-binding protein Lin28. *J Biol Chem* 283: 21310–21314

Piskounova E, Polytarchou C, Thornton JE, LaPierre RJ, Pothoulakis C, Hagan JP, Iliopoulos D, Gregory RI (2011) Lin28A and Lin28B inhibit let-7 microRNA biogenesis by distinct mechanisms. *Cell* 147: 1066–1079

Quinlan AR, Hall IM (2010) BEDTools: a flexible suite of utilities for comparing genomic features. *Bioinformatics* 26: 841–842

Reinhart BJ, Slack FJ, Basson M, Pasquienelll AE, Bettlnger JC, Rougvle AE, Horvitz HR, Ruvkun G (2000) The 21-nucleotide let-7 RNA regulates developmental timing in *Caenorhabditis elegans*. *Nature* 403: 901–906

Robinson JT, Thorvaldsdottir H, Winckler W, Guttman M, Lander ES, Getz G, Mesirov JP (2011) Integrative genomics viewer. *Nat Biotechnol* 29: 24–26

Roovers M, Hale C, Tricot C, Terns MP, Terns RM, Grosjean H, Droogmans L (2006) Formation of the conserved pseudouridine at position 55 in archaeal tRNA. *Nucleic Acids Res* 34: 4293–4301

Safra M, Nir R, Farouq D, Vainberg Slutskin I, Schwartz S (2017) TRUB1 is the predominant pseudouridine synthase acting on mammalian mRNA via a predictable and conserved code. *Genome Res* 27: 393–406

Schneider CA, Rasband WS, Eliceiri KW (2012) NIH Image to ImageJ: 25 years of image analysis. *Nat Methods* 9: 671–675

Schwartz S, Bernstein DA, Mumbach MR, Jovanovic M, Herbst RH, Leon-Ricardo BX, Engreitz JM, Guttman M, Satija R, Lander ES *et al* (2014) Transcriptome-wide mapping reveals widespread dynamic-regulated pseudouridylation of ncRNA and mRNA. *Cell* 159: 148–162

Schwinn MK, Machleidt T, Zimmerman K, Eggers CT, Dixon AS, Hurst R, Hall MP, Encell LP, Binkowski BF, Wood KV (2018) CRISPR-mediated tagging of endogenous proteins with a luminescent peptide. *ACS Chem Biol* 13: 467–474

Shen W, Le S, Li Y, Hu F (2016) SeqKit: a cross-platform and ultrafast toolkit for FASTA/Q file manipulation. *PLoS ONE* 11: e0163962

Song N, Ma X, Li H, Zhang Y, Wang X, Zhou P, Zhang X (2015) microRNA-107 functions as a candidate tumor suppressor gene in renal clear cell carcinoma involving multiple genes. *Urol Oncol* 33: 205.e1–205.e11.

Song J, Zhuang Y, Zhu C, Meng H, Lu B, Xie B, Peng J, Li M, Yi C (2019) Differential roles of human PUS10 in miRNA processing and tRNA pseudouridylation. *Nat Chem Biol* 16: 160–169

Sun C, Sang M, Li S, Sun X, Yang C, Xi Y, Wang L, Zhang F, Bi Y, Fu Y, et al. (2015) Hsa-miR-139-5p inhibits proliferation and causes apoptosis associated with down-regulation of c-Met. *Oncotarget* 637: 39756–39792

Sur S, Steele R, Shi X, Ray RB (2019) miRNA-29b Inhibits Prostate Tumor Growth and Induces Apoptosis by Increasing Bim Expression. *Cells* 8: 1455

Thomson JM, Newman M, Parker JS, Morin-Kensicki EM, Wright T, Hammond SM (2006) Extensive post-transcriptional regulation of microRNAs and its implications for cancer. *Genes Dev* 20: 2202–2207

Trabucchi M, Briata P, Garcia-Mayoral M, Haase AD, Filipowicz W, Ramos A, Gherzi R, Rosenfeld MG (2009) The RNA-binding protein KSRP promotes the biogenesis of a subset of microRNAs. *Nature* 459: 1010–1014

Treiber T, Treiber N, Plessmann U, Harlander S, Daiss JL, Eichner N, Lehmann G, Schall K, Urlaub H, Meister G (2017) A compendium of RNA-binding proteins that regulate microRNA biogenesis. *Mol Cell* 66: 270–284

Varambally S, Yu J, Laxman B, Rhodes DR, Mehra R, Tomlins SA, Shah RB, Chandran U, Monzon FA, Becich MJ *et al* (2005a) Integrative genomic and proteomic analysis of prostate cancer reveals signatures of metastatic progression. *Cancer Cell* 8: 393–406

Varambally S, Yu J, Laxman B, Rhodes DR, Mehra R, Tomlins SA, Shah RB, Chandran U, Monzon FA, Becich MJ *et al* (2005b) Gene Expression Omnibus GSE3325 (https://www.ncbi.nlm.nih.gov/geo/query/acc.cgi?acc=GSE3325). [DATASET]

Viswanathan SR, Daley GQ, Gregory RI (2008) Selective blockade of microRNA processing by Lin28. *Science* 320: 97–100

Wang L, Wang S, Li W (2012) RSeQC: quality control of RNA-seq experiments. *Bioinformatics* 28: 2184–2185

Wang XR, Luo H, Li HL, Cao L, Wang XF, Yan W, Wang YY, Zhang JX, Jiang T, Kang CS *et al* (2013) Overexpressed let-7a inhibits glioma cell malignancy by directly targeting K-ras, independently of PTEN. *Neuro Oncol* 15: 1491–1501

Wang BD, Ceniccola K, Yang Q, Andrawis R, Patel V, Ji Y, Rhim J, Olender J, Popratiloff A, Latham P *et al* (2015a) Identification and functional validation of reciprocal microRNA-mRNA pairings in African American prostate cancer disparities. *Clin Cancer Res* 21: 4970–4984

Wang BD, Ceniccola K, Yang Q, Andrawis R, Patel V, Ji Y, Rhim J, Olender J, Popratiloff A, Latham P *et al* (2015b) Gene Expression Omnibus GSE64333 (https://www.ncbi.nlm.nih.gov/geo/query/acc.cgi?acc=GSE64333). [DATASET]

Wightman B, Ha I, Ruvkun G (1993) Posttranscriptional regulation of the heterochronic gene lin-14 by lin-4 mediates temporal pattern formation in *C. elegans*. *Cell* 75: 855–862

Wolter JM, Kotagama K, Pierre-Bez AC, Firago M, Mangone M (2014) 3′LIFE: a functional assay to detect miRNA targets in high-throughput. *Nucleic Acids Res* 42: e132

Wolter JM, Kotagama K, Babb CS, Mangone M (2015) Detection of miRNA targets in high-throughput using the 3′LIFE assay. *J Vis Exp* 99: e52647

Wright JR, Keffer-Wilkes LC, Dobing SR, Kothe U (2011) Pre-steady-state kinetic analysis of the three *Escherichia coli* pseudouridine synthases TruB, TruA, and RluA reveals uniformly slow catalysis. *RNA* 17: 2074–2084

Yang X, Boehm JS, Yang X, Salehi-Ashtiani K, Hao T, Shen Y, Lubonja R, Thomas SR, Alkan O, Bhimdi T *et al* (2011) A public genome-scale lentiviral expression library of human ORFs. *Nat Methods* 8: 659–661

Yi R, Qin Y, Macara IG, Cullen BR (2003) Exportin-5 mediates the nuclear export of pre-microRNAs and short hairpin RNAs. *Genes Dev* 17: 3011–3016

Zeng Y, Yi R, Cullen BR (2005) Recognition and cleavage of primary microRNA precursors by the nuclear processing enzyme Drosha. *EMBO J* 24: 138–148

Zucchini C, Strippoli P, Biolchi A, Solmi R, Lenzi L, D'Addabbo P, Carinci P, Valvassori L (2003) The human TruB family of pseudouridine synthase genes, including the Dyskeratosis Congenita 1 gene and the novel member TRUB1. *Int J Mol Med* 11: 697–704